NAVAL POSTGRADUATE SCHOOL

MONTEREY, CALIFORNIA

THESIS

THE EFFECT OF FERROFLUID ON A DILATANT FLUID'S INTRUSION RESISTANCE

by

Joshua M. Strader

December 2020

Thesis Advisor: Abram H. Clark IV
Second Reader: Emil P. Kartalov

THIS PAGE INTENTIONALLY LEFT BLANK

REPORT DOCUMENTATION PAGE	*Form Approved OMB No. 0704-0188*

1. AGENCY USE ONLY *(Leave blank)*	**2. REPORT DATE** December 2020	**3. REPORT TYPE AND DATES COVERED** Master's thesis

4. TITLE AND SUBTITLE THE EFFECT OF FERROFLUID ON A DILATANT FLUID'S INTRUSION RESISTANCE	**5. FUNDING NUMBERS**
6. AUTHOR(S) Joshua M. Strader	
7. PERFORMING ORGANIZATION NAME(S) AND ADDRESS(ES) Naval Postgraduate School Monterey, CA 93943-5000	**8. PERFORMING ORGANIZATION REPORT NUMBER**
9. SPONSORING / MONITORING AGENCY NAME(S) AND ADDRESS(ES) Office of Naval Research, CA 93955	**10. SPONSORING / MONITORING AGENCY REPORT NUMBER**

11. SUPPLEMENTARY NOTES The views expressed in this thesis are those of the author and do not reflect the official policy or position of the Department of Defense or the U.S. Government.

12a. DISTRIBUTION / AVAILABILITY STATEMENT Approved for public release. Distribution is unlimited.	**12b. DISTRIBUTION CODE** A

13. ABSTRACT (maximum 200 words)

When small, macroscopic, solid particles (like glass beads or grains of starch) are immersed in Newtonian fluids (like water or glycerol), the resulting material demonstrates solidification under sudden driving, like from intrusion of an object above a threshold velocity. The physical means for this effect are not fully understood. One mechanism that has been proposed involves hydrodynamic pressure: the fluid must flow through the pore structure between particles as the material deforms. Consistent with this picture, the viscosity of the fluid has been identified as a contributing factor to this resistance. The ability to control the viscosity in real time would allow for maximum resistive pressure when needed and then for low resistance in between periods of high driving. One possibility for accomplishing this is using ferrofluids. Ferrofluids contain molecules of iron coated in a surfactant and suspended in a solvent. This mixture is capable of changing its viscosity when a magnetic field is present. I will explore the mechanical properties, including the impact resistance, where the simple Newtonian fluid is replaced with a ferrofluid. I compare this with existing data in literature and from previous projects in our group. I find that the experimental results match predicted theory to a point and then data suggests that other forces counteract these predictions. I find that ferrofluids are capable of creating a tunable complex fluid mixture and warrant further research.

14. SUBJECT TERMS ferrofluid, Newtonian, non-Newtonian, dilatant, hydrodynamic pressure	**15. NUMBER OF PAGES** 63
	16. PRICE CODE

17. SECURITY CLASSIFICATION OF REPORT	**18. SECURITY CLASSIFICATION OF THIS PAGE**	**19. SECURITY CLASSIFICATION OF ABSTRACT**	**20. LIMITATION OF ABSTRACT**
Unclassified	Unclassified	Unclassified	UU

NSN 7540-01-280-5500 Standard Form 298 (Rev. 2-89) Prescribed by ANSI Std. 239-18

THIS PAGE INTENTIONALLY LEFT BLANK

Approved for public release. Distribution is unlimited.

THE EFFECT OF FERROFLUID ON A DILATANT FLUID'S INTRUSION RESISTANCE

Joshua M. Strader
Major, United States Army
BS, University of Alaska Fairbanks, 2013

Submitted in partial fulfillment of the
requirements for the degree of

MASTER OF SCIENCE IN COMBAT SYSTEMS TECHNOLOGY

from the

NAVAL POSTGRADUATE SCHOOL
December 2020

Approved by: Abram H. Clark IV
Advisor

Emil P. Kartalov
Second Reader

Kevin B. Smith
Chair, Department of Physics

THIS PAGE INTENTIONALLY LEFT BLANK

ABSTRACT

When small, macroscopic, solid particles (like glass beads or grains of starch) are immersed in Newtonian fluids (like water or glycerol), the resulting material demonstrates solidification under sudden driving, like from intrusion of an object above a threshold velocity. The physical means for this effect are not fully understood. One mechanism that has been proposed involves hydrodynamic pressure: the fluid must flow through the pore structure between particles as the material deforms. Consistent with this picture, the viscosity of the fluid has been identified as a contributing factor to this resistance. The ability to control the viscosity in real time would allow for maximum resistive pressure when needed and then for low resistance in between periods of high driving. One possibility for accomplishing this is using ferrofluids. Ferrofluids contain molecules of iron coated in a surfactant and suspended in a solvent. This mixture is capable of changing its viscosity when a magnetic field is present. I will explore the mechanical properties, including the impact resistance, where the simple Newtonian fluid is replaced with a ferrofluid. I compare this with existing data in literature and from previous projects in our group. I find that the experimental results match predicted theory to a point and then data suggests that other forces counteract these predictions. I find that ferrofluids are capable of creating a tunable complex fluid mixture and warrant further research.

THIS PAGE INTENTIONALLY LEFT BLANK

TABLE OF CONTENTS

THIS PAGE INTENTIONALLY LEFT BLANK

LIST OF FIGURES

LIST OF ACRONYMS AND ABBREVIATIONS

cP	Centipoises
DST	discontinuous shear thickening
FEMM	Finite Element Method Magnetics
Gees	multiple of g-force
g-force	force opposing acceleration (1 gravitational unit)
mT	MiliTesla (1/1000 of a Tesla)
SEM	Scanning Electron Microscopy

THIS PAGE INTENTIONALLY LEFT BLANK

ACKNOWLEDGMENTS

I want to express my sincere appreciation for the time and effort that Professor Abe Clark put into making sure my thesis was a success. Unlike many other thesis advisors, Professor Clark allowed me the latitude to test an idea I had. By being a mentor through this process, he enabled me to achieve one of my life goals. Contributing to the body of scientific knowledge, however small, enables us all to move toward a better future. I am very grateful to have had this opportunity. A special thanks to Professor Dragoslav Grbovic for the amazing Scanning Electron Microscope photos. Additionally, I want to thank all the professors that endured my many questions. Finally, I want to thank my wife, Rachel, and family for understanding my extended absence over the past several months.

THIS PAGE INTENTIONALLY LEFT BLANK

I. INTRODUCTION

A. COMPLEX FLUIDS

Complex fluids are fluids with physical properties that make them behave in unexpected ways. Often, they are non-Newtonian, meaning they are not well described by a Newtonian rheology, where stresses scale linearly with strain rate. The viscosity, which is the ratio of stress to strain rate, is a constant material parameter. A Newtonian rheology captures many common fluids over a wide range of strain rates. In non-Newtonian fluids, the ratio of stress to strain rate is not a constant but varies with system properties, including sometimes dramatically with strain rate. These nonlinear effect can manifest macroscopically in ways that can make it seem like the material is both solid-like and fluid-like. This could be useful in wide range of applications such as, motion dampening systems or lower speed fragmentation protection. For example, at impact pressures over a certain threshold a non-Newtonian fluid responds by stiffening against the pressure like a solid. If the impact pressure is under a certain threshold a non-Newtonian fluid moves around the intruding object more like a fluid. There are many other applications that could make use of a fluid that can respond to pressures exerted on the system, like propulsion systems. One simple way to make a complex fluid is to add solid particles to an otherwise Newtonian fluid [1]. Figure 1 illustrates one such a system and the components that are considered when creating a non-Newtonian response.

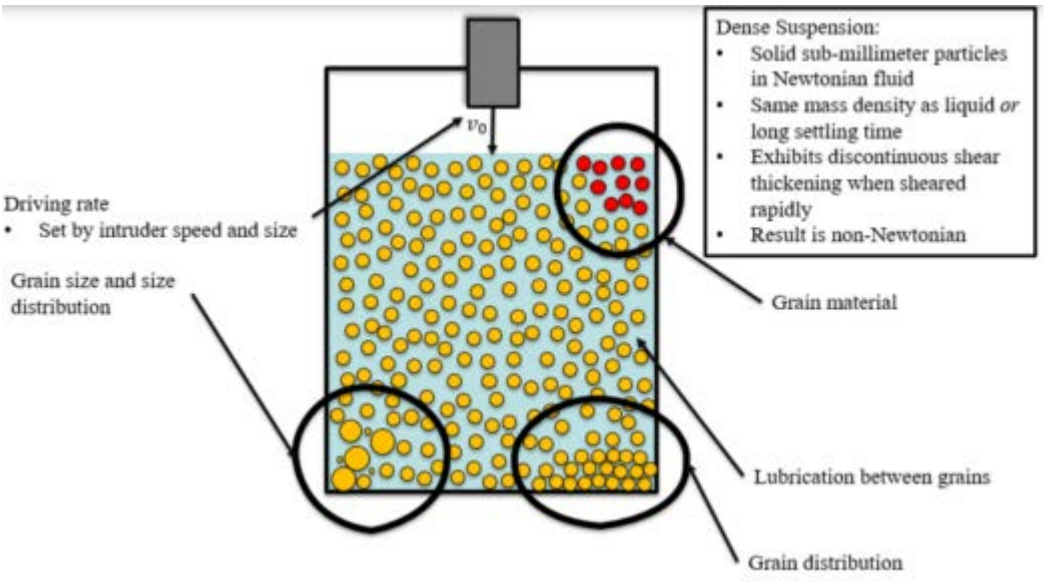

Figure 1. Dense Suspension Illustration. Source: [2].

When the particle volume fraction (ϕ) is small the mixture still behaves as a simple Newtonian fluid, with a constant viscosity η_f that increases with ϕ. When the concentration of solid particles becomes large enough, several nonlinear physical effects take over, and the macroscopic behavior is highly nonlinear or non-Newtonian. Oobleck is one example of this, typically made using cornstarch particles, which are very small (1-10 microns), irregularly shaped, and mixed with water. This organic molecule may have some surface chemistry effects that play a role in this response. There have been several demonstrations of the properties of Oobleck and experimental data collected on the substance, but there is not a lot known on the exact mechanism that causes this change in shear resistance. A combination of organic [3], physical [1], and hydrostatic [4] explanations have been explored.

This behavior is also observed with non-organic particles in similar systems, such as water and glass micro-spherical particles. Thus, it is likely that important aspects of the behavior are controlled by fluid-mechanical effects as well as some other effects that are fundamentally related to the granular solid phase. However, the fundamental physical processes that give rise to the complex response of these materials is still a subject of debate. In previous research [1] a theory was put forward that Darcy flow, where fluid is

pushed through a porous material, plays a dominant role in determining the flow response of a particle-fluid mixture in the limit where the particles are densely packed (that is, making solid-solid contact with each other and not suspended). This theory describes the material response for densely packed particles submerged in fluid and then applies this description to predict the dynamics of low- to moderate-speed impacts. In particular, it makes specific, quantitative predictions regarding the role viscosity as well as various intruder characteristics. However, these predictions have never been tested. One goal of this thesis work is to specifically test these predictions.

B. FERROFLUIDS

How the material response changes for different fluid viscosities is important to understand complex fluids that use ferrofluids. Ferrofluids are a mixture of a solvent and surfactant coated iron particles that when exposed to a magnetic field exhibit a change in fluid viscosity. When exposed to a magnetic field the ferromagnetic iron particles become magnetized and attract to each other. This attraction leads to a macroscopic change in viscosity. As shown in Figure 2 the structure of the iron particles in the ferrofluid is similar to cornstarch, but the particles themselves are much smaller than cornstarch particles (10 nanometers compared to 1-10 micrometers). Additionally, the iron particles typically occupy a very small amount of the fluid volume (roughly 10%).

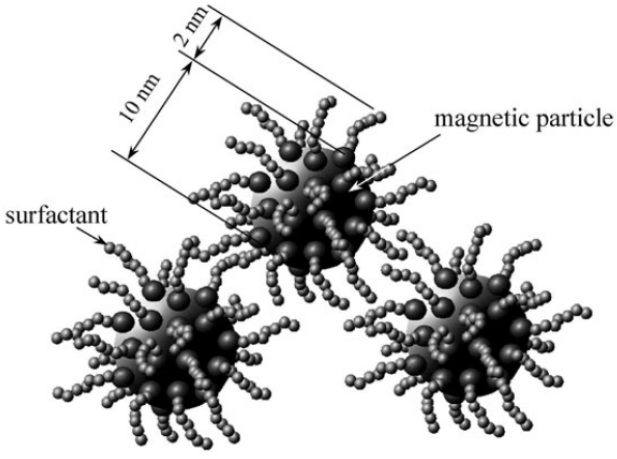

Figure 2. Schematic View of Coated Magnetic Particles in a Ferrofluid. Source: [5].

This ability to change viscosity has found uses in the automotive industry in shock absorbers and the electronics industry in speaker coils. Recent experiments have shown further medical applications by manipulating ferrofluids using a magnetic field to control its movements in vitro [6]. Combining the ability to change viscosity, the possibility of containment using a magnetic field, and the non-Newtonian behavior of complex fluids opens up the possibility of a tunable, magnetically contained complex fluid that exhibits a non-Newtonian response to impact or other sudden mechanical loading. This could be done by creating a uniform magnetic field and applying it to a mixture of ferrofluid and solid particles, effectively changing the viscosity of the fluid with no other manipulations to the system.

C. TUNABLE-DENSE FLUIDS

The area of tunable particle-fluid mixtures is largely unexplored, partly due to the fact that the mechanisms leading to non-Newtonian behavior in fluid-particle mixtures are not completely explained. For example, the role of viscosity, which can be tuned in a ferrofluid, has not been fully tested. A simple explanation might be that, at a fixed strain rate, the effective viscosity of the fluid-particle mixture increases linearly with the viscosity of the Newtonian fluid. Therefore, using a fluid that has a viscosity that can be changed by a magnetic field would allow the tuning of resistive pressure that could be generated during some deformation. Characterizing and understanding the capabilities of such a material may allow for the ease of liquid movement with an increased resistive response when required. Furthermore, such a suspension may be constrainable without the need of a physical container. In benchtop explorations I conducted, Figure 3, a ferrofluid and glass spherical mixtures displays a liquid type nature when on a piece of Plexiglas. It will flow around the surface pulling the suspended particles within it around. When exposed to a permanent magnet the mixture becomes more solid in appearance and no longer flows like a liquid, but slides like a solid across the surface to maintain itself within the magnetic field.

Left: fluid-like, no magnetic field; right: solid-like, magnetic field present

Figure 3. Ferrofluid Mixture Movement without/with a Magnetic Field

Understanding the characteristics of this kind of materials could allow for responsive and moldable fragmentation armor, more flexible damping systems, and other applications were an elongating of impact forces could reduce overall stresses on materials. The goal of this thesis is to explore the possibility of using ferrofluids as the liquid component of non-Newtonian fluid-particle mixture. The main idea is that external magnetic fields will alter the viscosity, which should in turn effect macroscopic material behavior. This thesis reviews literature on dense particle-fluid mixtures; covers experimental data results for such mixtures made with a water-glycerol mix, to test the role of viscosity, as well as ferrofluids in the presence of magnetic fields; and presents quantitative analysis of the recorded results. Our main conclusions are that viscosity plays a role in setting the macroscopic behavior, and that increasing the magnetic field is analogous to increasing the viscosity for complex fluids made using ferrofluids. However, we find that large viscosities begin to decrease the macroscopic stresses, in contradiction to previous theoretical predictions.

THIS PAGE INTENTIONALLY LEFT BLANK

II. BACKGROUND

A. GENERAL BEHAVIOR OF PARTICLE-FLUID MIXTURES

Systems of solid particles, with sizes on the scale of 1-100 micrometers, placed into a Newtonian fluid are common in a variety of engineering and geophysical contexts. The rheology, meaning the mathematical description of the flow behavior, varies strongly with the volume fraction occupied by the particles. For small particle volume fraction ϕ (typically $\phi < 0.4$), the suspension behaves as a Newtonian fluid, with a constant viscosity that increases with ϕ. For $\phi > \phi_J$ (typically $\phi_J \sim 0.6$), the particles are jammed [7,8], and the material behaves as a yield-stress solid [1]. In between these two limits (typically $0.4 < \phi < 0.6$), the viscosity increases dramatically if the shear rate exceeds some critical value, the value of which depends on [1] and other microscopic features. This behavior, called shear thickening or sometimes discontinuous shear thickening (DST), arises from some combination of granular effects, like jamming [7,8] and Reynolds dilatancy [9]; Fluid-related phenomena, like Darcy flow [9,10] and lubrication [4]; and possibly surface chemistry of the particles [3].

B. USING SATURATED GRANULAR BEDS TO PROBE THE BEHAVIOR

Not surprisingly, recent work [9] has shown that similar behavior arises in a bed of particles fully immersed in a fluid. In this system, a bed of particles is loaded by gravity and totally immersed in a fluid. Particles are making solid-solid contact, at least at the beginning before any external driving takes place. This is the dense limit of a suspension, and it has many similar properties and can act like a solid under rapid driving. Rapidly driven dense suspensions will almost always have a part of the material where the particles are densely packed and making solid-solid contact. Therefore, a saturated granular bed serves as a useful model system to investigate certain generic features of particle-fluid mixtures. Additionally, this system is interesting in its own right from a physics and engineering perspective.

The primary theoretical work in this thesis is based on a recent paper by Jerome et al. [9]. These authors proposed a theory of the rheology of saturated granular beds primarily based on Reynolds dilatancy and Darcy flow. Reynolds dilatancy refers to the fact that granular materials can dilate or compact when sheared, and Darcy flow refers to the flow resistance of a viscous fluid that is pushed through a porous medium. They then used these theories to make predictions about the dynamics of moderate-speed impacts by an intruder into the saturated granular bed. Although impact was used in their paper and will be used in this thesis, the results concern general flow behavior of the material. These authors explicitly tested the role of the initial density of the particle phase (i.e., Reynolds), but they did not explicitly show data for particle size or fluid viscosity (i.e., Darcy).

C. DARCY-REYNOLDS THEORY APPLIED TO IMPACTS

The theory from Jerome et al. [9]. was developed to explain the response to impact of fluid-saturated particle beds. During initial impact, the material experience shear deformations which can cause the particle phase to dilate. If this occurs, the pore structure in between the particles will expand, and more fluid must be sucked into these larger voids. This process will be governed by Darcy flow, which describes the flow of a fluid through a porous medium. The Darcy equation is Equation (1):

$$q = -\frac{\kappa}{\eta_f}\Delta p \tag{1}$$

where flow rate (q) is related to permeability (κ), viscosity (η_f), and the pressure gradient (Δp)[9]. Rearranging Equation (1) gives Equation (2):

$$-q\frac{\eta_f}{\kappa} = \Delta p \tag{2}$$

and predicts if the viscosity is the only variable that increases so does the pressure gradient. The permeability scales as the pore size squared, and therefore scales here as the particle size squared [9,10].

The strength of the material response is also related to how much the particle phase must dilate during shear: a more densely packed particle phase should mean that more dilation is necessary and therefore a stronger fluid response. An experiment by Jerome et al. was conducted to test this by dropping a solid sphere on a suspended matrix and recording the observed reactions. Altering the density of the particles, ϕ, by packing them closer together allowed them to reduce the size of the pores between solids and test the response of the suspension [9]. The packing fraction was controlled by first fluidizing the suspension using an upward fluid flow and then tapping the container side to induce settling. The amount of settling was controlled by the number of taps. They recorded the fluid pressure under the impact with a hydrophone and low frequency sensor. The general method set up is outlined in Figure 4.

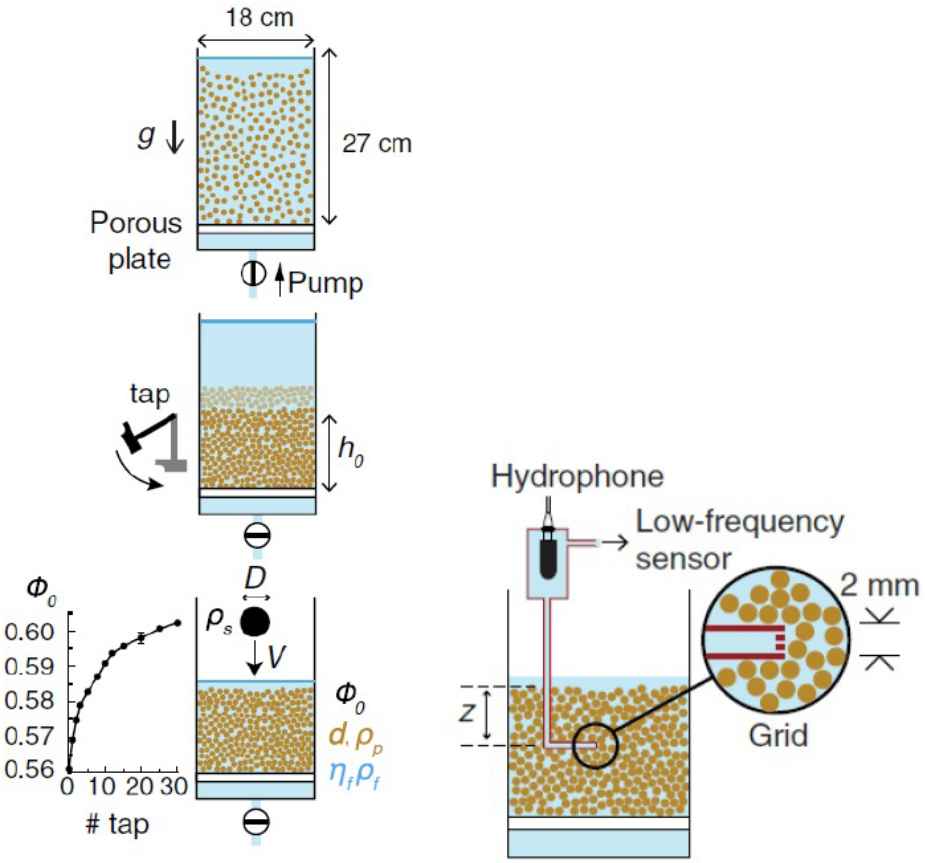

Figure 4. Methods Set Up Used in the Jerome et. al Experiments. Adapted from [9].

During this experiment loose compaction and dense compaction were tested. An example of loose compaction was demonstrated with a packing fraction of 0.560, and an example of dense compaction was demonstrated with packing fraction of 0.604. Reynolds theory predicts that the loose packing will want to compact during impact and the denser packing will want to dilate during impact. They found results that supported this hypothesis: a positive pressure peak for loose compaction and a negative pressure peak for dense compaction. The transition point was located between the compaction zones at 0.585. After completing this experiment, they modeled pore pressure (P_f) as in Equation (3):

$$P_f = -\frac{\eta_f}{\kappa}\alpha V_p(\phi - \phi_c)L \tag{3}$$

where viscosity (η_f), permeability (κ), first order constant (α), velocity scale (V_p), initial packing fraction (ϕ), settled packing fraction (ϕ_c), and the deformation length scale (L) and is not dependent on the impactor diameter (D) or impact velocity (υ). Here $\kappa \propto d^2$ and d is the diameter of the beads. This predicts that the experienced deformation should decrease with an increase in viscosity. However, they did not show results for testing η_f and κ. We will test them here.

D. CONNECTING RHEOLOGY TO IMPACT DYNAMICS

Equation (3) describes pore pressure, but how this relates to impact is not obvious. For example, the length scale *L* would increase with time after impact, since a larger portion of the ball will be in contact with the material. Jerome et al. showed that this length scale $L = \alpha$, the contact radius, will be approximately given by $\alpha^2 = D\delta$, where δ is the penetration depth, during the initial stages of impact (a small-angle approximation is used for this result). If the pore pressure due to Equation (3) is the dominant force acting on the contact area between the ball and the material, Newton's second law can be written in Equation (4).

$$\rho_s(\pi D^3/6)\ddot{\delta} = \pi a^2 A P_f \tag{4}$$

Equation (5) can then be derived by plugging in everything and integrating once.

$$d\tilde{\delta}/d\tilde{t} = -(2/5)\tilde{\delta}^{5/2} + 1 \tag{5}$$

Equation (6) is used to define the time aspect of Equation (5).

$$t_m = \frac{D}{V}(\lambda\Delta\phi)^{-2/5} \tag{6}$$

Where $\tilde{\delta} = \delta/(Vt_m)$ is the dimensionless penetration and $\tilde{t} = t/t_m$ is the dimensionless time.

Thus, the Darcy-Reynolds theory makes specific predictions about how the forces on a ball during impact should scale with various material properties, including particle size and fluid viscosity. These scaling laws have never been tested; in Jerome et al. [9], only the role of ϕ was tested.

E. PREVIOUS EXPERIMENTS

Previous experiments from our lab recorded results on how the forces scale with particle size. These experiments utilized a freely falling mass to impact such dense suspensions and used both accelerometer data and high speed video analysis to characterize how changing the variables effects the overall system reaction. In previous experimental work by Neil Causley [11], which is precursor work to the work presented here, a saturated granular bed was impacted by an intruding mass. This work tested the diameter of the particles in the granular material. This relates to the predictions of Jerome et. al equations, since κ is proportional to the diameter of the beads squared [9]. Figure 5 shows the experimental set up of Causley, which is the basis of the experimental set up executed during my experimentation.

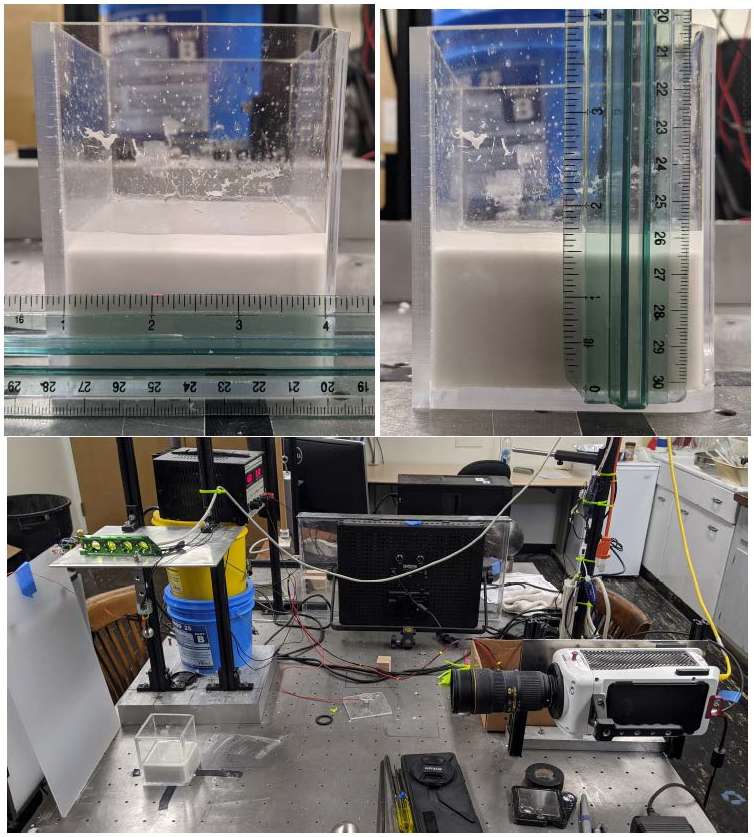

Top: Granular bed in the container used for drop testing. Bottom: Overview of experimental rig, including camera and magnetic drop mechanism.

Figure 5. Saturated Granular Bed Experiments. Source: [11].

Causley used microspheres that ranged from 53-850 μm submerged in water and the intruder was dropped from 1-20 centimeters. An accelerometer, recording at 5,000 Hertz, and high speed camera was used to capture the impacts. The packing fraction (ϕ) was determined by using the volume (V), and density (ρ) of both the water ($_f$) and glass microspheres ($_g$). In matching the fluid density (ρ_f) to the density of the microspheres (ρ_g) he found that $\rho_f \approx \rho_g$. This allowed the Equation (8) to be used for ϕ

$$\phi = \frac{V_g}{V_g + V_f} \tag{7}$$

and observed strong impact response at $\phi = 0.6$ for the soda lime microspheres [11].

Causley performed impact tests for a range of particle sizes. He found that the peak forces on the ball during impact scaled as $F_{max} = Av_0^{\alpha}$, where $\alpha \approx 1.4$ and $A \propto d^{\beta}$ with $\beta \approx -0.8$. The Darcy-Reynolds theory, Equation (1), would naively predict $\beta \approx -2$, but the results were not consistent with this. However, as we show in the Results section, $\beta \approx -0.8$ is consistent with the Darcy-Reynolds equation applied to impact of a sphere, as discussed in Equation (5). Figure 6 shows how *A* relates to *d*.

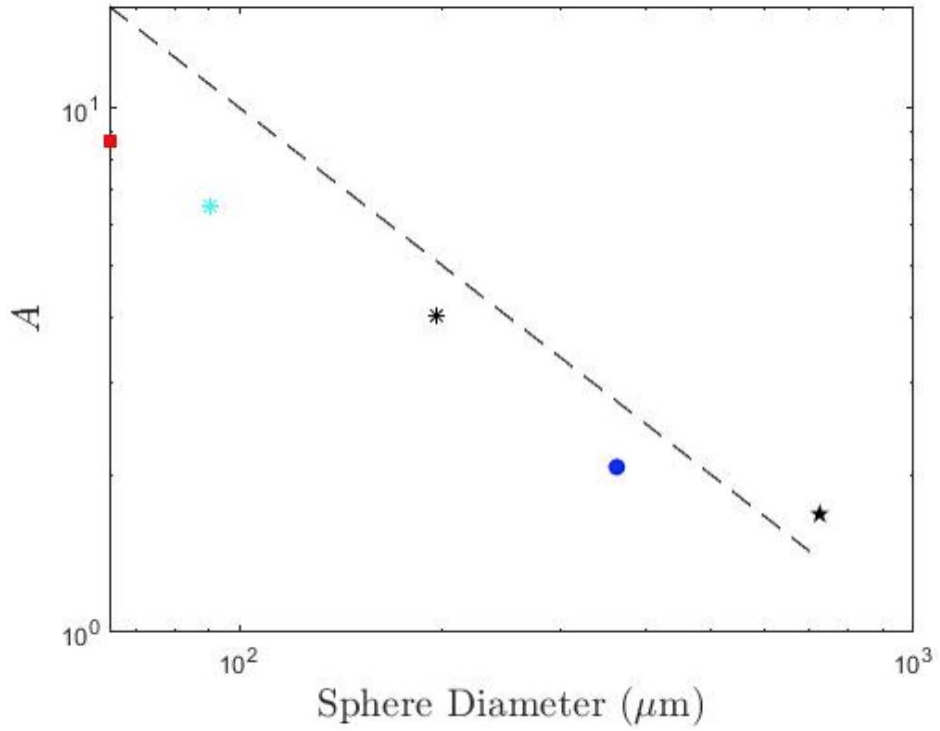

Scaling factor A versus mean microsphere diameter where the $53–75\mu m$ microspheres are represented by a red square, $75–106\mu m$ microspheres is the cyan asterisk, $180–212\mu m$ microspheres is the black asterisk, $300–42\mu m$ microspheres is the blue circle, and $600–850\mu m$ microspheres is the black star. The dashed line represents a slope of -1; the data does not decrease as sharply as this, suggesting that the correct slope is closer to 0.8.

Figure 6. Sphere Diameter Impact on the Proportionality Constant Source: [11].

F. FERROFLUIDS

A ferrofluid is a "stable colloidal suspension of paramagnetic nano-particles in a liquid carrier. The particles, which typically have an average size of about 10 nm, are coated with a stabilizing dispersing agent (surfactant) which prevents particle agglomeration even when a strong magnetic field gradient is applied to the ferrofluid" [12]. The result is an increase in viscosity in the presence of magnetic field. Figure 7 shows how the viscosity of a ferrofluid changes with an increase in magnetic field.

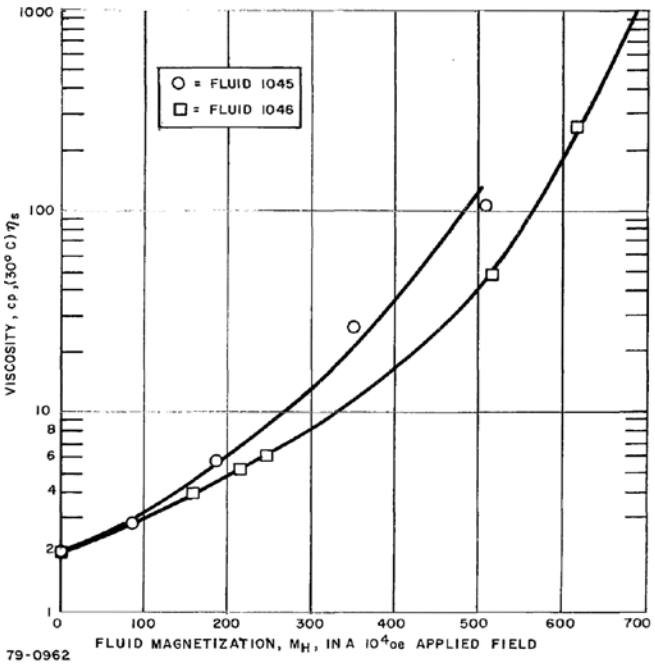

Figure 7. Viscosity/Magnetization Properties of HFPO Hexamer Acid. Source: [13].

Ferrofluids do experience a plateau in the magnetization as flux density increases. Research conducted by Rajesh Patel et al. [14]. found the magnetic saturation occurs at 258 Gauss for the tested ferrofluid. Figure 8 shows that $\approx 70\%$ of the effect can be achieved between 0 and 30 mT, which is the range we probe.

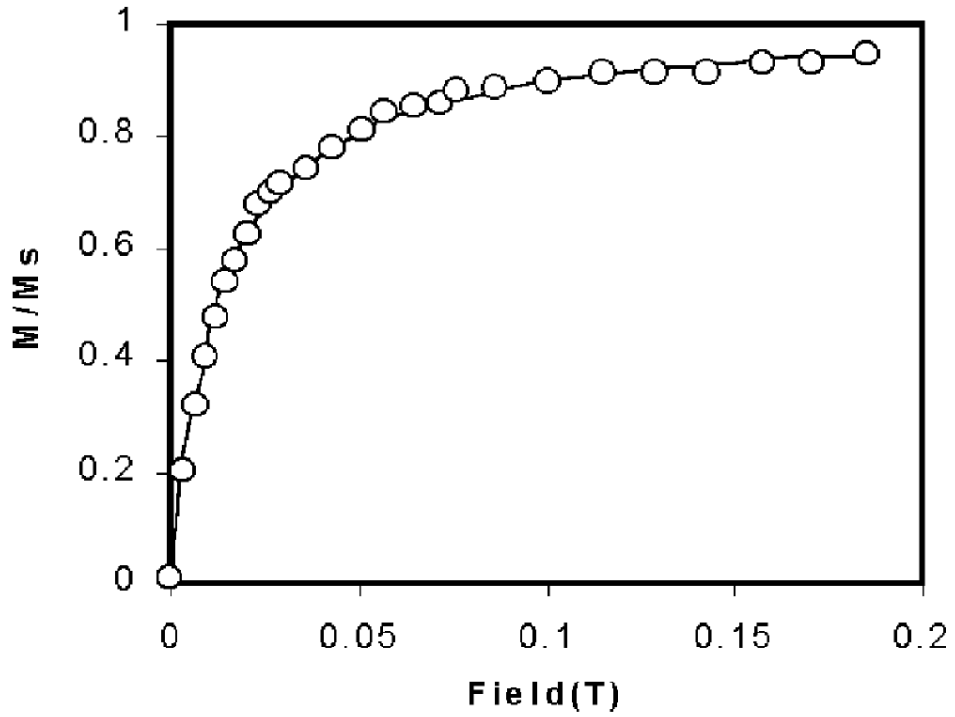

Figure 8. Reduced Magnetization Versus Magnetic Field for Fe3O4 Fluid.
Source: [14].

Each ferrofluid is a dynamic system that retains most fluid characteristics of the carrier fluid outside of a magnetic field. In a magnetic field viscosity is dependent on the particle diameter, size of surfactant layer, field strength, and original carrier fluid viscosity [13]. This ability to change the viscosity, combined with the Darcy-Reynolds theory discussed in the previous section, suggests the possibility of a magnetically tunable non-Newtonian type fluid. In addition to testing Darcy-Reynolds theory directly, we will show results of ferrofluids mixed with glass beads in the presence of magnetic fields to test the feasibility of magnetically tunable non-Newtonian type fluids.

THIS PAGE INTENTIONALLY LEFT BLANK

III. METHODS

A. INSTRUMENTATION

Experiments where conducted on granular beds using only $75-106\mu m$ soda lime microsphere as the solid. The microspheres have a compression strength of over 40,000 psi [15]. This provides adequate structural integrity for repeated impacts into the same mixture. The mixture was changed out by rinsing in tap water to remove all liquid parts of the mixture utilizing a mesh strainer of 45 micrometers, then drying. This allows for possible broken microsphere particles to be washed through and for larger remaining particles to be mixed throughout to minimize impact on the mixture. The liquid portion of the suspension was altered using both glycerol with tap water added to vary viscosity and ferrofluid. The ferrofluid mixture was ran with unused beads as the solids and carrier fluid would become lodged in the beads. The drop heights varied from 0.005-0.64 meters (measure by standard ruler) and the impactor was a 0.02 meter (measured with calipers) round stainless steel ball. The accelerometer was recorded at a refresh rate of 5,000 Hertz and had a max range of 200 times the gravitational acceleration.

B. MASS AND DROP HEIGHT FOR ACCELERATION

Altering the length of the drop increased the acceleration at the gravitational rate and impact velocity was calculated using the drop height. The accelerometer captured the rate of deceleration as a voltage change along the horizontal axis through a National Instruments LabView program. The resulting impact voltages where compared against the maximum g-force of the sensor to obtain peak deceleration. The rise time over which the impact occurred was recorded with the accelerometer and then analyzed using MATLAB. Finding the time for the start of impact was done by recording the constant voltage at each run and then finding the first increase over voltage noise in the sensor. The peak of the impact was found by isolating a length of time after the initial impact and finding the maximum value. This code was then checked individually to ensure that aberrations in the data were not included. Noise caused from the threaded rod striking the side of the container was identified manually and removed from the scope of the data.

C. VISCOSITY OF GLYCEROL-WATER MIXTURES

Utilizing glycerol and its established change in viscosity when diluted by water enabled a controlled response only varying in viscosity. Figure 9 shows the viscosity of a glycerol and water mixture by percentage of glycerol to water.

TABLE VI. COMPARISON OF VISCOSITY DATA

Glycerol, %	Viscosity, Centipoises: Authors 20° C.	Authors 30° C.	Sheely (16) 20° C.	Sheely (16) % diff.	Sheely (16) 30° C.	Sheely (16) % diff.	Archbutt and Deeley (2) 20° C.	Archbutt and Deeley (2) % diff.
0	1.005	0.8007	1.005	0.00	0.800	0.088	1.005	0.00
10	1.31	1.03	1.311	0.076	1.024	−0.058	1.328	1.37
20	1.76	1.35	1.769	0.51	1.360	0.74	1.798	2.16
30	2.50	1.87	2.501	0.04	1.876	0.32	2.529	1.16
40	3.72	2.72	3.750	0.81	2.731	0.40	3.718	−0.05
50	6.00	4.21	6.050	0.83	4.247	0.88	5.994	−0.10
60	10.8	7.19	10.96	1.48	7.312	1.70	10.791	−0.08
65	15.2	9.85	15.54	2.24	10.02	1.73	15.26	0.39
70	22.5	14.1	22.94	1.95	14.32	1.56	22.63	0.58
75	35.5	21.2	36.46	2.71	21.68	2.26	36.63	3.18
80	60.1	33.9	62.00	3.16	34.92	3.01	61.27	1.94
85	109	58.0	112.9	3.58	60.05	3.54	112.1	2.84
90	219	109	234.6	7.12	115.3	5.77	233.1	6.45
91	259	127	278.4	7.50	134.4	5.82	275.9	6.54
92	310	147	328.4	5.93	156.5	6.46	326.2	5.23
93	367	172	387.7	5.65	182.8	6.28	386.6	5.35
94	437	202	457.7	4.74	212.0	4.95	457.8	4.76
95	523	237	545	4.40	248.8	4.98	548.0	4.79
96	624	281	661	5.93	296.7	5.59	659.3	5.67
97	765	340	805	5.23	354.0	4.12	804.1	5.11
98	939	409	974	3.73	424.0	3.67	997.4	6.22
99	1150	500	1197	4.09	511.0	2.20	...	...
100	1412	612	1499	6.32	624.0	1.96	...	...

Three different experiments are captured by J.B. Segur and Helen E. Oberstar when comparing their glycerol to water mixtures viscosities.

Figure 9. Glycerol Aqueous Solution Viscosity. Source: [16].

When conducting this experiment to ensure that the proper packing fraction was maintained my mixture was by volume. Using the data provided in Figure 9 and a by using Origin 6.1, a fit was created, Figure 10, allowing viscosity to be calculated at all percentage values.

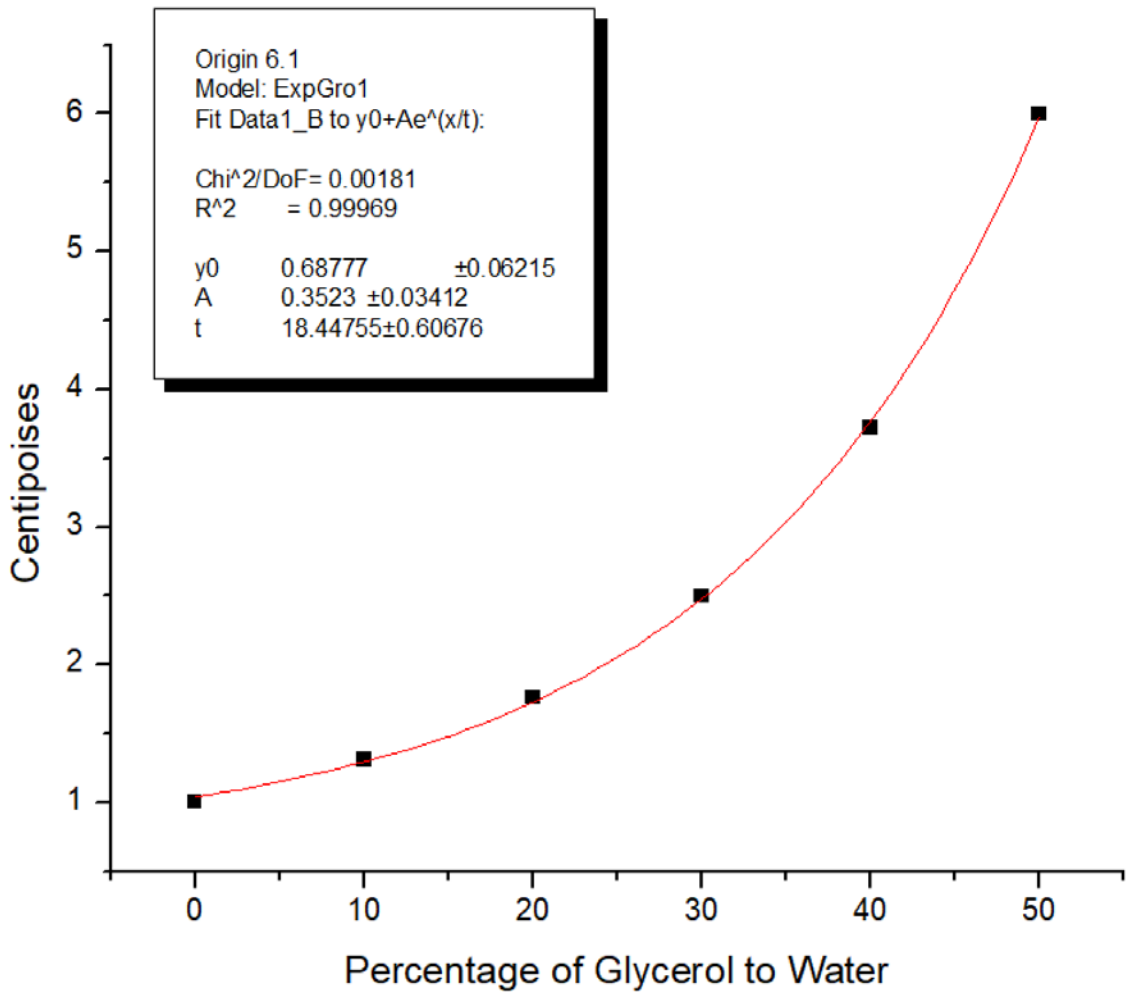

Figure 10. Centipoises vs. Percentage of Glycerol in Water

Because the ferrofluids contains iron particles that align in the magnetic field using glycerol as a viscosity varying substance allows for isolation of responses for comparison.

D. MAGNETIC FIELD

Creating a magnetic field to alter the viscosity of the ferrofluid was first done using Finite Element Method Magnetics (FEMM) modeling and then constructed. Using a 6" PVC pipe as the structure and 18 AWG copper wire a solenoid was constructed with a cut out section for the test vessel. Figure 11 show the solenoid wrapped with tape to reduce liquids ejected by the experiment from getting in between the wires.

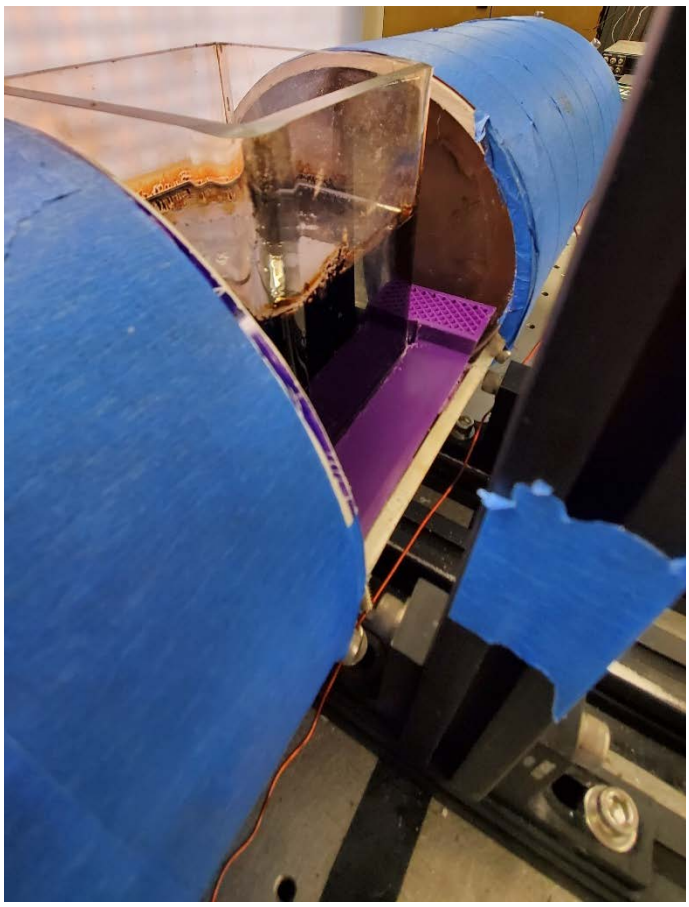

Figure 11. Solenoid with Ferrofluid Mixture

The solenoid had 1” thick filling of varying iron materials placed on either side of the cut out and held in place by Plexiglas to increase the magnetic flux. Iron materials used included iron sand and round and square iron bar stock. This was done to help decrease experienced eddy currents that would detract from the overall field. Additionally, to increase the field further permanent magnets where used in varying position with the solenoid to achieve the desired magnetic field. The field was tested with a Hall Probe and overall uniformity in the area of the test sample from center to outside edge. The background noise of the instrument was recorded and subtracted from all other field values. The maximum Amperes that could be created by the power source was 6.3 Amps. This created a 3 miliTesla (mT) field and was the lowest magnetic flux that was tested. Using combinations of magnets and solenoid current, additional fields of 9 mT, 14mT, and 31 mT were created as measured at the impact site. The ferrofluid used here has a magnetic

saturation point of 44 mT [17], meaning that we cover most of the range of this particular ferrofluid.

E. MAKING THE TEST BED

The dense mixture was made the same way for glycerol and ferrofluid mixtures. A 60% packing fraction (ϕ) was used in previous experiments and to enable easier correlation the mixture was made by the same method [11], to achieve the same packing fraction. The goal is to make a granular phase that repeatedly dilates by the same amount, thereby isolating the role of other effects in Equations (3) through (6). Fluid was added and stirred slowly to ensure that mixture was complete and the test container had a homogenous mix and no pockets of dry particles or areas of just fluid. The one zone that was only fluid was $\approx 1mm$ layer on top of the particles. This helped ensure that all settling was visible in how clear the top layer was. This also ensured that all particles where in liquid during the experiment. Divots created by the impact where filled by moving particles from the outside edge towards the middle and then waiting for the particles to settle again before the next drop.

F. DETAILS OF IMPACT EXPERIMENTS

The drops where recorded by LabView through the accelerometer and high speed video was triggered by the same program. An electromagnet held the impactor in place until a command was given to drop in LabView. Triggering the drop stopped the current flow to the electromagnet and triggered the high speed camera to save the recorded footage. The accelerometer was attached to National Instruments voltage recorder using 32 AWG copper wire. A minimum free falling mass of wire was maintained by securing excess wire to the drop apparatus, so only the amount of wire required to reach the end of the impact was free. A 48-gram stainless steel ball was threaded to a 3.5” threaded iron rod and the accelerometer was attached to the threaded iron rod. After each drop the excess material that was attached to the ball was cleaned off and the footage was reviewed to ensure the impact occurred primarily on the gravitational axis. The height was recorded using a standard ruler from the bottom of the ball to the top of the mixture. The high speed footage

was recorded using a Phantom v711 and was backlit, as in Figure 12, to provide a distinct contrast between the ball and background.

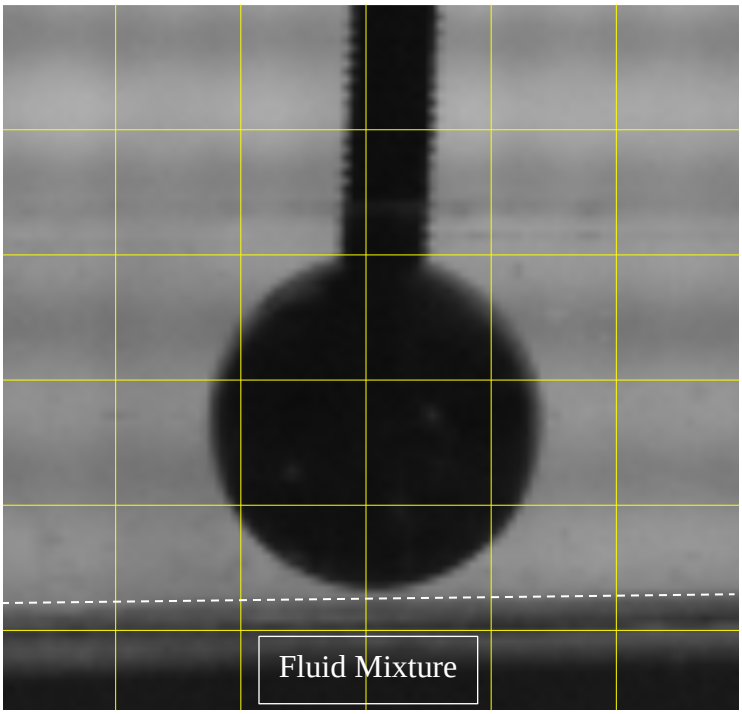

Figure 12. High Speed Camera Contrast Example

Accelerometer data was reviewed, after the video confirmed that the impact had occurred properly. Accelerometer data was checked to ensure that the time from before drop initiation to after a complete stop was recorded.

When running tests, a series of drops took between 30 to 60 minutes. The temperature in the lab was recorded continuously over the testing period for the glycerol drops with an average of 23˚ C. The range of temperature was between 21.7˚ C and 24.4˚ C and was recorded to ensure that temperature variance of the room would not affect the glycerol viscosity. All experiments were conducted on the same day, generally within 4 hours from time of mixing until last run. This was done to ensure that the tendency of water to evaporate and glycerol's hydroscopic nature did not impact viscosity over the length of

the experiment ferrofluid has an evaporating rate of <0.01 [17], but when preparing the experiment, it was noticed that over long periods of time the mixture of both fluids and particles seemed to dry out. Settling experiments were conducted to ensure that a four-hour time window was adequate to prevent settling of the overall suspension that could affect the test. Figure 13 shows that several hours of settling do not significantly impact the results of the experiment. Days of settling did cause the material to respond differently, however.

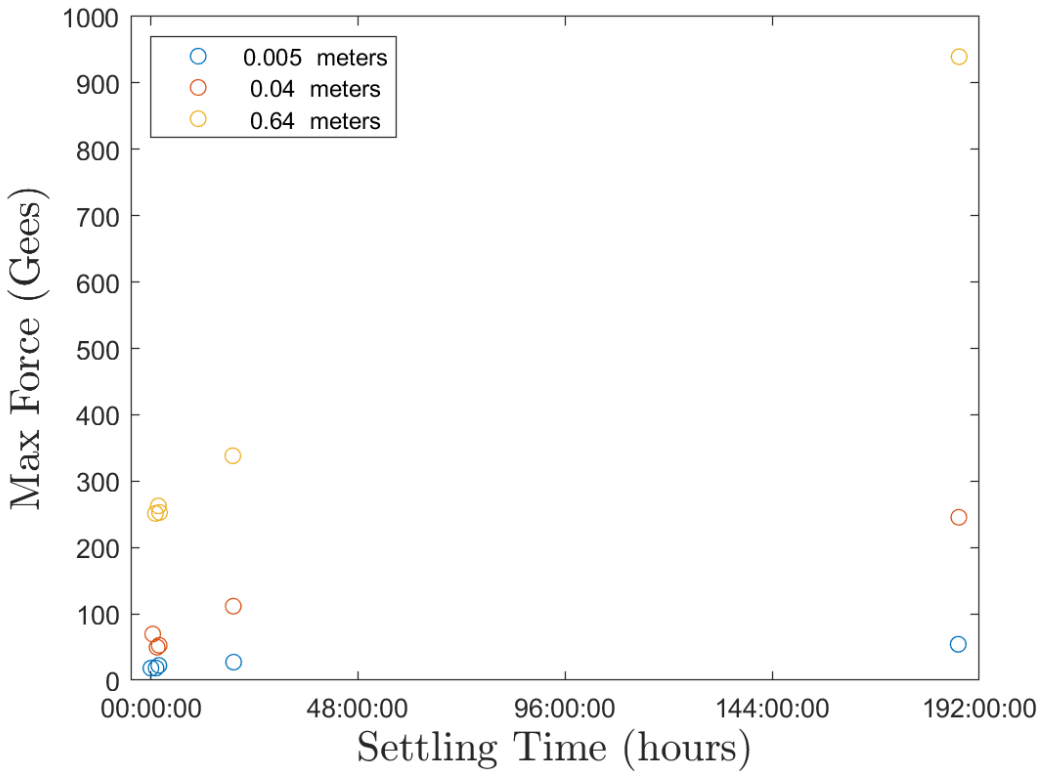

Figure 13. Settling Time Experiments

Figure 13 illustrates how the impact forces can change if no agitation of the dense suspension is conducted. Avoiding this in the ferrofluid was conducted by thoroughly mixing the suspension and then allowing time to settle to a state of dense suspension. To ensure that the ferrofluid volume remained as constant as possible it was placed in a refrigerator when not being used. It was also warmed to room temperature before each set of experiments.

G. EXTRACTING QUANTITATIVE DATA

Data processing was done by extracting the gravitational axis accelerometer data. Running a code that would identify the first rise above the noise and then capturing the entire impact event to include several hundred frames after returning to a noise state. The code results were reviewed for each individual run to ensure that code had properly identified the initiation and cut off points of the relevant impact. Occasionally, the impact created by the threaded steel rod with the sides of the container would create a spike that interfered and this was manually edited out of the analyzed data.

IV. RESULTS

This chapter shows the results of the data collected during the impacts into the dense suspension with both glycerol and ferrofluids. We find that the direction of the Jerome et al. [9]. predictions hold up, to a point. Once a certain threshold of viscosity is passed the predictions made not only change in value, but in direction. A prediction using Darcy flow analysis would suggest that at higher values of viscosity the experienced forces of an intruding mass would continue to increase as viscosity increases. However, we find that at a critical viscosity, the observed behavior is not consistent with this prediction and the intruder forces decrease.

A. DATA COLLECTION

Data from our impact studies was collected using an accelerometer connected through LabView. The sample rate was set to 5,000 samples per second and three channels of data was collected, one channel per directional axis. Data collected on the Y and Z axis was not used in the calculations performed via MATLAB. The data from the direction of impact, the X axis, was imported into MATLAB and processed by converting the voltage output of the accelerometer into a proportional force. In Figure 14 the raw data is represented by the voltage readout over time. We can see that a peak voltage was approximately 1.86 volts and by using the maximum voltage output and the maximum gravitational force for this sensor, the corresponding value of force can be calculated.

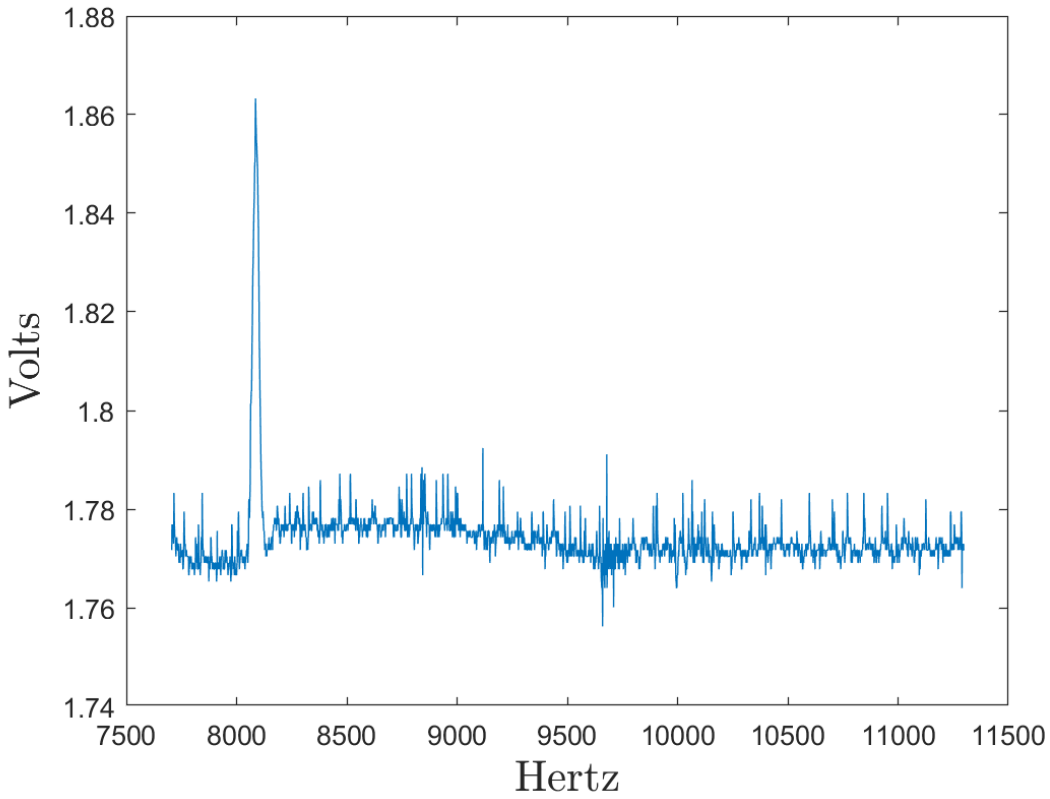

The time axis is equal to 5,000 Hz or 1 second = 5,000 units on the X axis.

Figure 14. X Axis Voltage Over Time

Using MATLAB the relevant data is trimmed, identifying the start and end of the signal related to the impact. Figure 15 shows that if the rod that held the accelerometer struck the sides; the maximum peak might have to be addressed manually to ensure the correct forces were being evaluated.

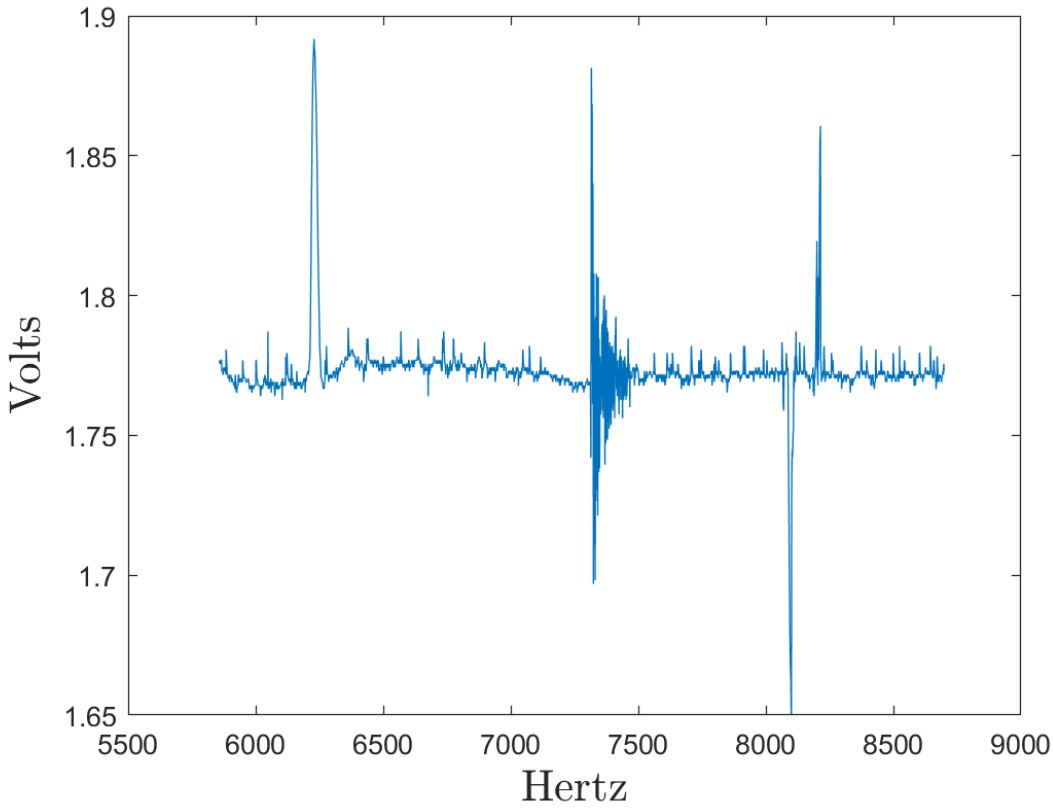

Figure 15. X Axis Voltage Over Time with Strikes on the Container

The strikes to the side of the container are visible after the impact of the ball. In this case the maximum value is still the investigated impact and the data calculations are unaffected. In cases where the maximum value was due to side strikes the data points from that strike are removed.

B. PREDICTING IMPACT RESULTS USING DARCY-REYNOLDS THEORY

Darcy flow and Reynolds dilatancy provide the structure for how the pore pressure model that was used by Jerome et al. [9]. study. Using this previous work, we examine the equation of motion to develop theoretical predictions for how peak forces should depend on system parameters. Although the equation of motion was developed by Jerome et al., they did not analyze or test how forces during impact depend on system parameters. According to the analysis discussed in the background section, culminating in Equation (6), the dimensionless velocity is always 1, meaning that the dimensionless peak acceleration

is always constant. As shown in Equation (9), the dimensionless peak acceleration is multiplied by the length unit divided by two time units to obtain the dimensional peak acceleration.

$$a_{\max} = \tilde{a}_{\max} \cdot \frac{\delta_m}{t_m^{\,2}} \rightarrow \frac{V t_m}{t_m^{\,2}} \rightarrow \frac{V}{t_m} \tag{8}$$

Then, by inserting the expression for t_m in terms of the ball diameter (D), the fluid viscosity (η_f), the particle diameter (d), the permeability of the material(κ), the packing fraction (ϕ), an unknown constant (α), the density of the fluid(ρ), an effective friction coefficient (A), and intruder mass (M), the dimensional peak acceleration can be written as shown in Equation (10).

$$a_{\max} \propto V \frac{V}{D} \cdot (6A\alpha \frac{\eta_f D}{\rho \kappa V} \Delta\phi)^{\frac{2}{5}} \tag{9}$$

Solving Equation (11) for η_f gives the power of each of the characteristics found in Equation (11).

$$a_{\max} \propto V^{1.6} D^{-0.6} \eta^{0.4} d^{-0.8} M^{-0.4} \tag{10}$$

Having this solved allows us to use the data collected and compare it to this prediction. Additionally, referencing the works conducted by Causley [11]; he finds that d scales not with Equation (3) directly, which would predict $\frac{1}{d^2}$, but more closely to $\frac{1}{d}$, and even closer to $d^{-0.8}$. This is consistent with Equation (11), which was derived for impact of a spherical intruder and takes into account the fact that the contact area is changing as the sphere penetrates. Additionally, Causley found that forces scale as $V^{1.4}$, which is similar to the predicted scaling of $V^{1.6}$. For the present work, we note that Equation (11) also predicts that the peak force should scale with viscosity as $\eta_f^{0.4}$.

C. GLYCEROL

Using varying concentrations of glycerol, the viscosity was changed and experimental data collected over the range of impact speeds. In Figure 16 we show the acceleration measured by the accelerometer as a function of time for impacts with similar speeds into mixtures with varying viscosities. The bead size remained constant throughout the entirety of all experiments conducted.

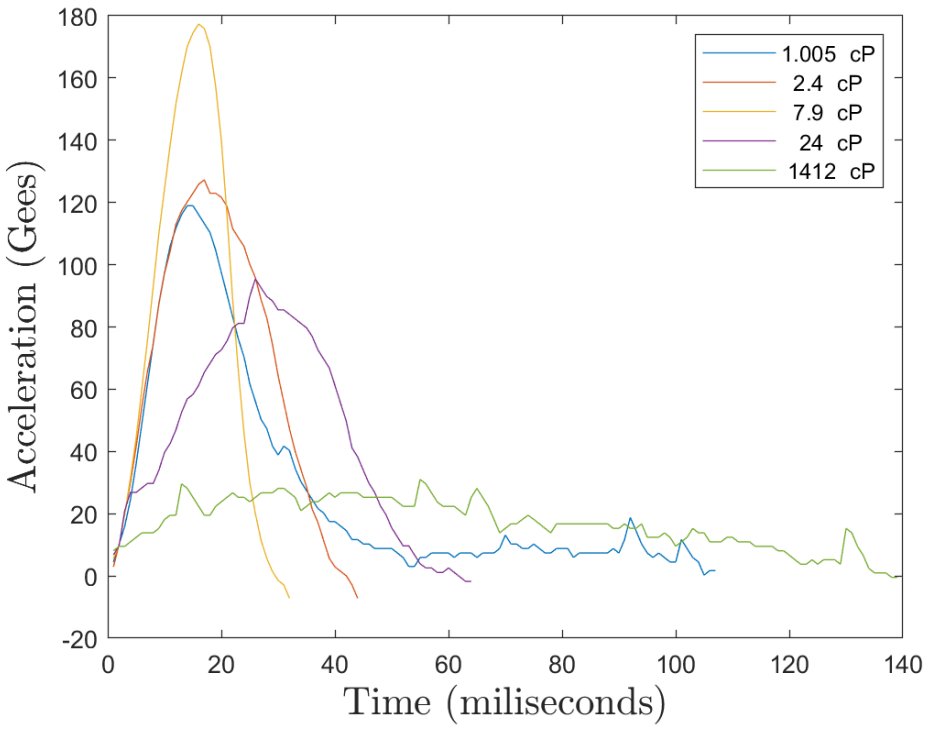

The 1.005 cP value is taken from work done by Causley and was conducted from the height of 0.03m. The rest of the data was collected from a 0.02m drop. Because we are trying to compare the characteristic profile and acceleration this drop height was suitable for comparison.

Figure 16. Viscosity Dependent Acceleration

The data for 1.005 cP is from experiments conducted by Causley [11] and shares both the experimental design and bead size and type. We can see that as predicted in Jerome et al. [9]. the forces experienced increase with viscosity up to 7.9 cP, but then start to decline. Surprisingly, this data shows that the forces increase with increasing viscosity at

first, but then begin to decrease for viscosities larger than 7.9 cP. As the viscosity increases over 7.9 cP the time of the impact lengthens to a value over four times as long at the highest cP value of 1412 cP, or 100% glycerol.

Figure 17 shows the value of the peak plotted as a function of speed for each viscosity. Different symbol colors represent different viscosities (in order of increasing viscosity: blue, red, yellow, purple, green), where symbol colors are the same as shown in Figure (16).

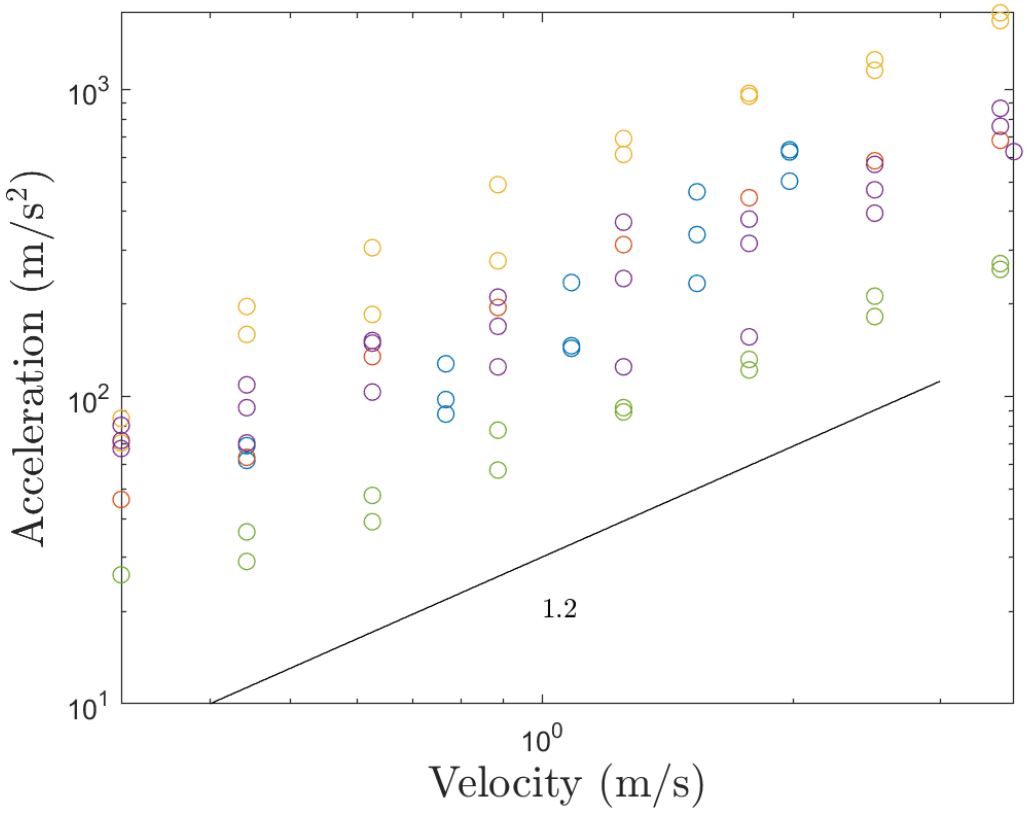

Figure 17. Acceleration Versus Impact Velocity

Figure 17 shows that the trend in Figure 16 holds for all impacts: increasing viscosity leads to increasing force and shorter time scales until 7.9 cP, and then forces decrease and time scales increase for larger viscosities. We perform power-law fits of the form $a_{max} = Av_0^{\alpha}$ to

the data shown in Figure 17, and we plot the magnitude *A* as a function of viscosity in Figure 18.

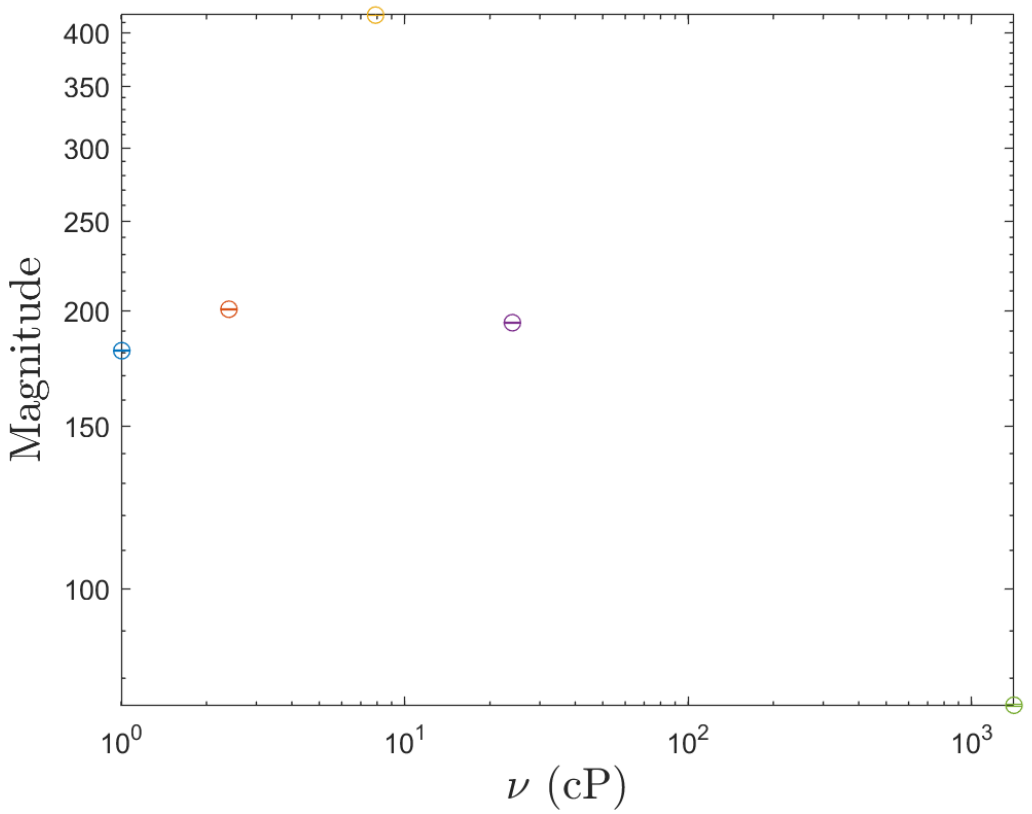

Figure 18. Magnitude of Impact versus Viscosity

Figure 18 again reiterates our result: peak forces tend to increase up to a viscosity of about 10 cP, and then decrease as the viscosity is further increased. This does not agree with the theory from Jerome et al. This is the first major result of this thesis. Equation (11) predicts a velocity power of 1.6 as viscosity increases, but we see values more related to 1.2. This discrepancy in the velocity dependence could have many sources, such as inertial, other viscous, or gravitational effects, all of which are disregarded here. In Figure 19 we see that the value of 1.2 fits all but one inside the experimental error and the value for 1412 cP is closely related.

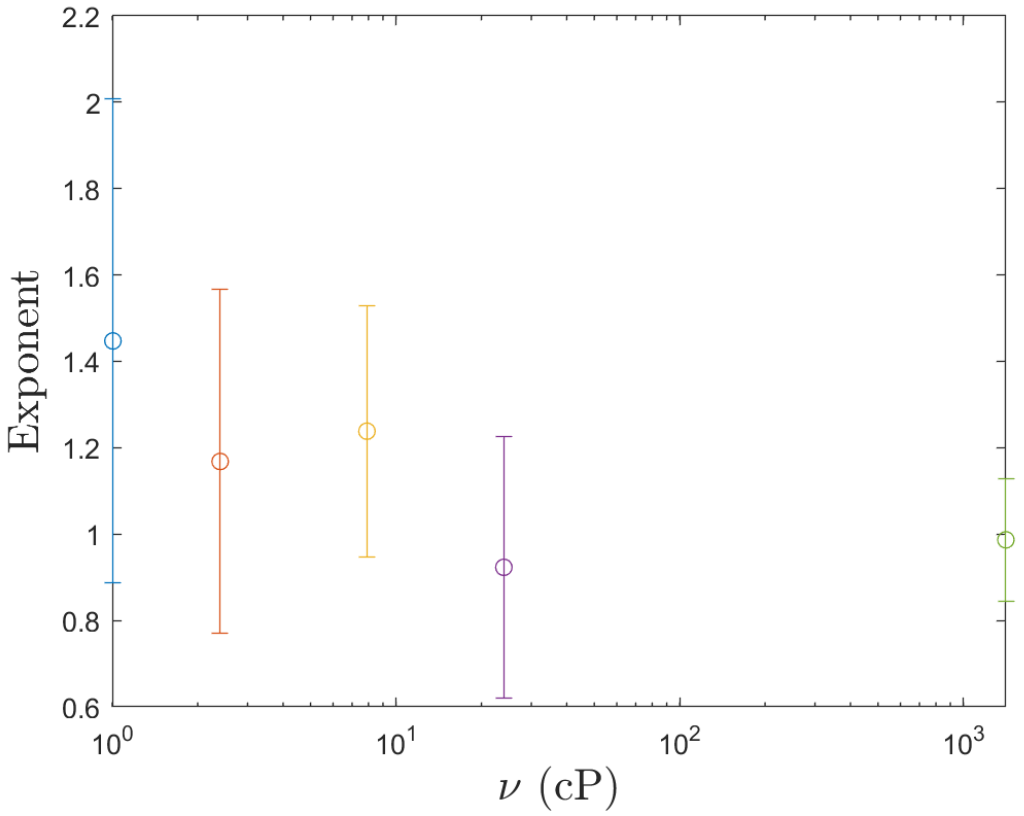

Figure 19. Exponential Power of Viscosity with Respect to Acceleration and Velocity

The fact that forces increase only up to about 10 cP and then begin to decrease might suggest that the viscosity is playing more of a lubrication role at higher viscosities, allowing particles to move by each other with less collisions occurring. In Equation (10) A and α in the theory were just frictional and unknown constants, but that these may depend on viscosity. If particles cannot make solid-solid contact, then the frictional properties of the material as a whole will be greatly reduced [18]. The reduction in frictional forces allows the intruding mass to move through the mix over a greater amount of time spreading out the forces of impact. Figure 20 shows the material frictional coefficient compared effective frictional coefficient.

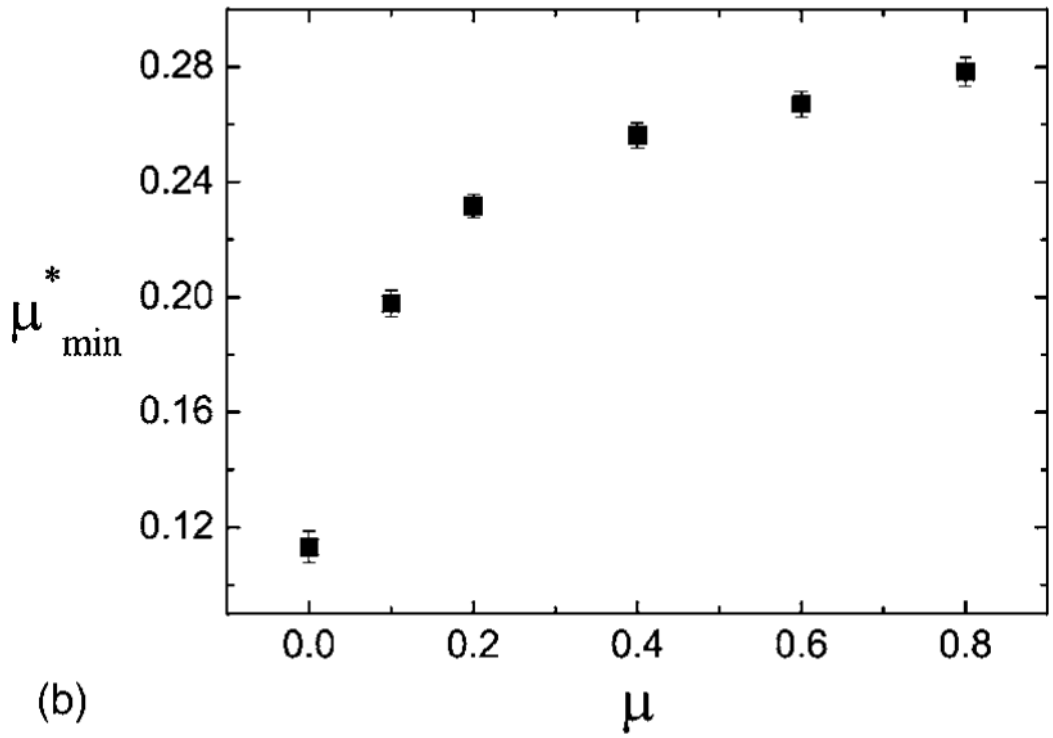

Figure 20. Frictional Properties in the Quasistatic Regime. Adapted from [18].

Figure 20 shows that effective friction of a particulate material is effectively lower in a dry mixture when the friction of grains is not present. In our system, large viscosities may prevent the particles from making solid-to-solid contacts that would generate frictional forces between grains. Simply, the beads flow around each other more than they interact frictionally with each other. This mechanism may help explain why large viscosities lead to smaller forces..

D. FERROFLUID

Similar experiments were also conducted on saturated granular bed of the same beads sizes and material, but with ferrofluid instead of glycerol. The ferrofluid is shown with results alongside the magnetic field that was used during testing. The rheometry of the ferrofluid was also intended to be conducted using a traditional rheometer at University of California at Santa Cruz, but due to COVID pandemic no viscosity measurements were able to be taken. Instead the data sheet [17] states that the viscosity of the ferrofluid without

a magnetic field is 6 cP and we expect one order of magnitude of maximum achievable cP. For the purposes of this experiment the field strength is an acceptable representation of equivalent viscosity. We know from previous experimental data that as the field strength increases so does the viscosity [13,14]. Figure 21 shows that for each value of mT we did achieve different impact profiles, which further supports that the increases in magnetic field strength were adequate to alter the viscosity of the fluid.

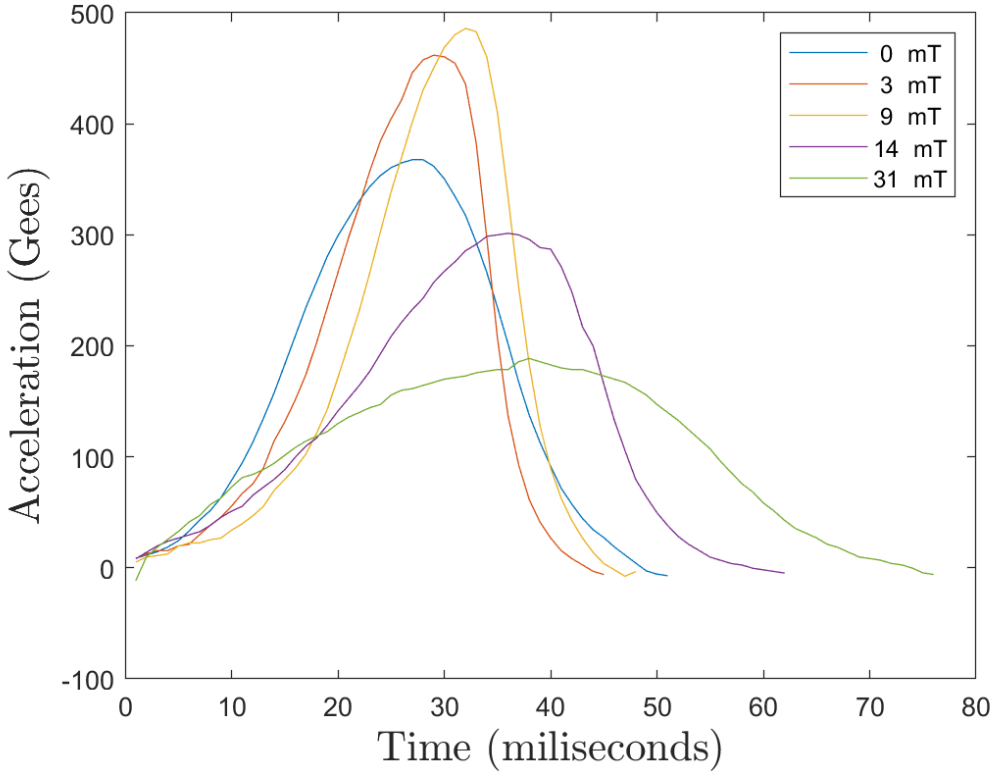

This figure is from a drop height of 0.16 meters, because the heights at and below 0.02 meters where not testable at 31 mT. The magnetic field was strong enough to overcome the drop setup and pull the ball into the side of the container.

Figure 21. Tesla Dependent Acceleration

Figure 21 shows a value of 9 mT as the highest impact forces while both lower and higher values of magnetic field lower as the field increases and decreases. This suggest that if that the 9 mT point is close to the 7.9 cP point as either a lower or higher viscosity value results in decreased forces. The saturation point for this ferrofluid is 44mT [17] and the

magnetization curves of Figure 8 show that most of the magnetization occurs in the beginning of the range of magnetic fields studied here. This aligns well with the expectation that the viscosity value for 9 mT should reside closer to the middle of the range of viscosity rather than to either side of the range. As before, we explore in Figure 22 the values of the peak plotted as a function of speed for each viscosity (different symbol colors).

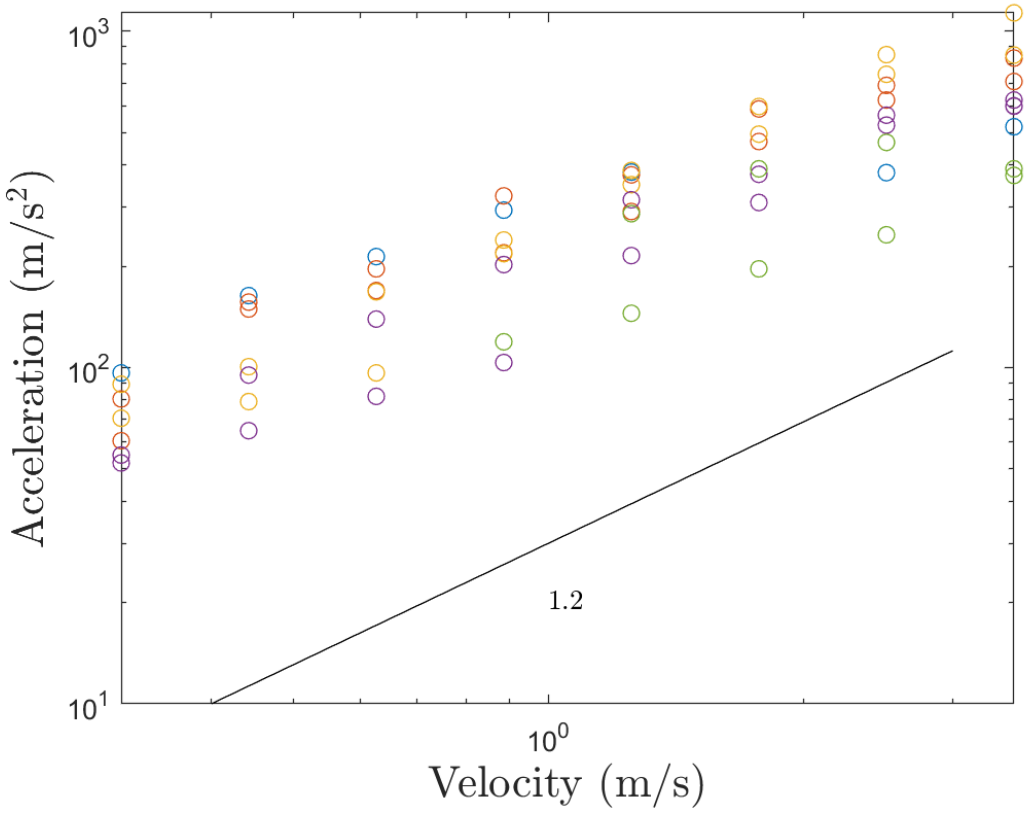

Figure 22. Acceleration versus Velocity in Ferrofluid

When we evaluate acceleration over the velocities again for ferrofluid and Figure 21 shows us that the previously found value of 1.2 is similar. We also see that the values increase as the velocity increases as previously demonstrated. Then comparing these magnitudes to the magnetic field we get Figure 23.

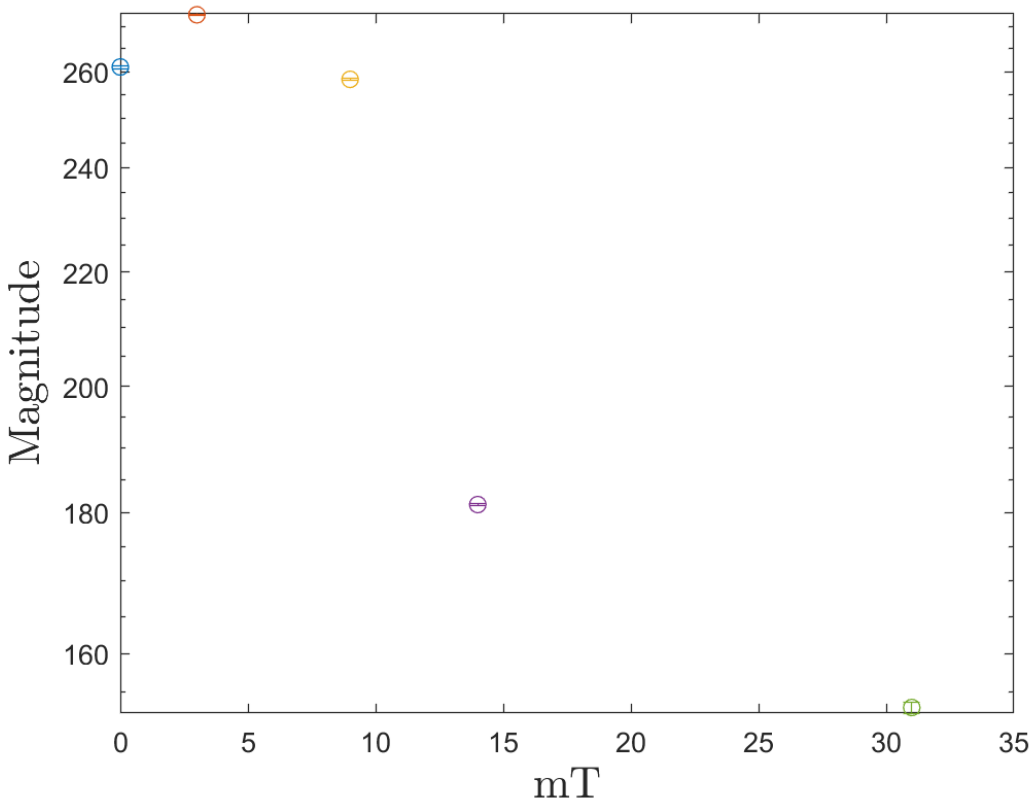

Figure 23. Magnitude of Impact versus Tesla

We see again that there is a characteristic high point with a decrease in magnitude as the magnetic field increases. This suggests that the magnetic fields available were adequate to represent how this dynamic changes across the range of viscosities. Figure 24 plots the error versus magnitude of the exponent and magnetic field.

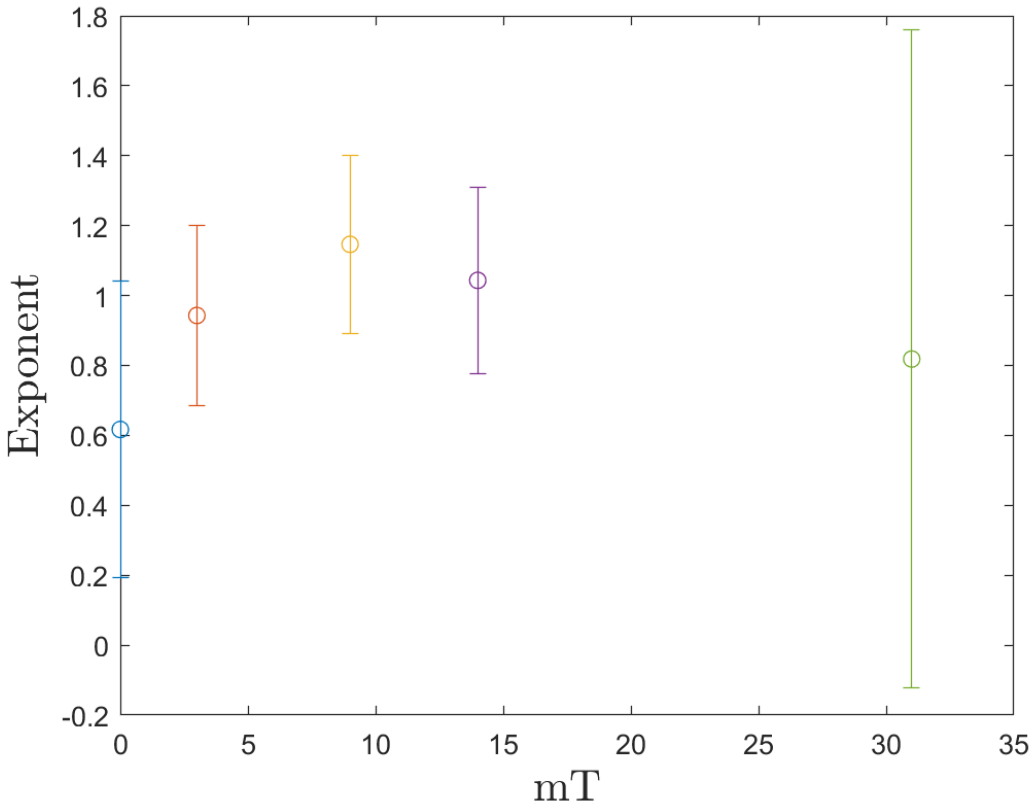

Figure 24. Exponent of Force versus Tesla

Again we see that exponent value holds near 1 through all values of magnetic field. This suggest that similar forces are responsible for both the glycerol suspensions and the ferrofluid suspensions. It also suggests that by utilizing the magnetoviscous properties of ferrofluid we could tune and predict the impact characteristics of a dense suspension. However, increasing the fluid viscosity only led to larger forces up to a point, as with the glycerol experiments and in contradiction to the theoretical predictions.

E. MAGNETIC FLUID

Ensuring that the ferrofluid was behaving like a simple viscous fluid in the mixture was a concern, since it was not known how the iron particles might interact with the glass beads during repeated deformations. This was addressed using scanning electron microscopy of samples before and after impacts. By removing the carrier fluid via a

hotplate, the ferrofluid mixture was prepared and scanned. Figure 25 shows the result of this process.

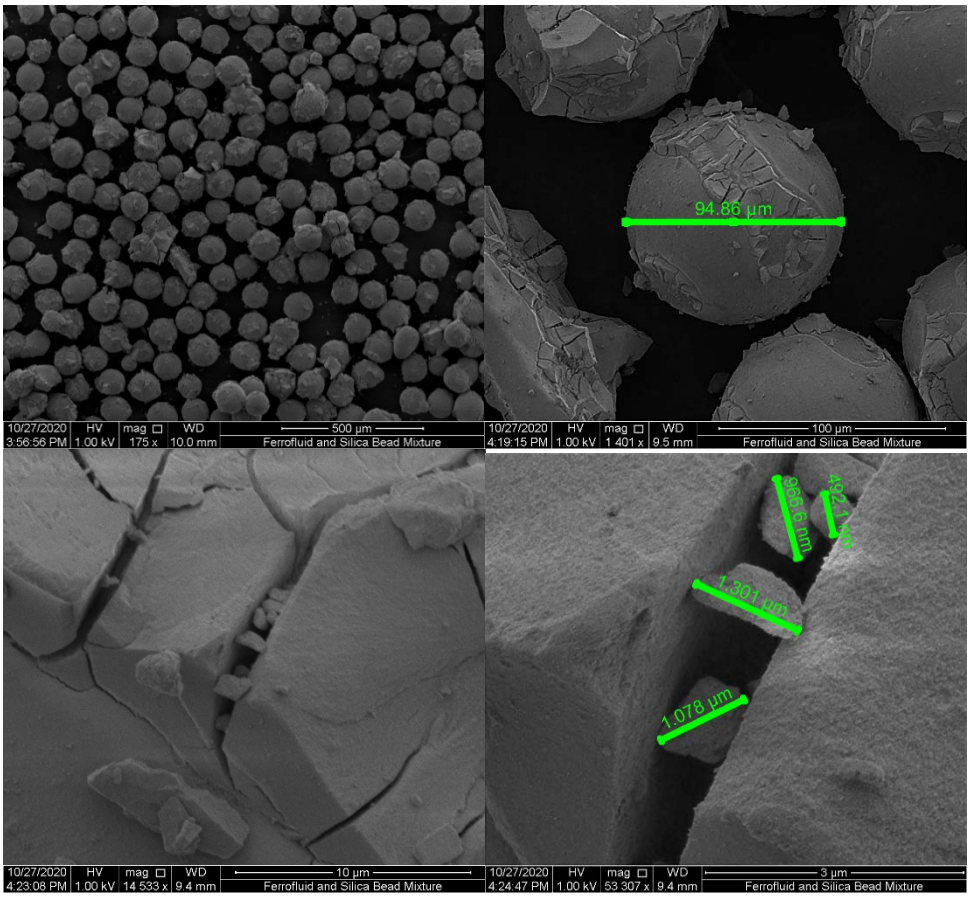

Figure 25. Dry Ferrofluid Silica Bead Mixture. Source: [19].

We can see that the ferrofluid solids, which are approximately 12 nanometers, gather around and cling to the silica beads when dried. The surfactant is designed to keep the iron particles from agglomerating with each other while suspended in the carrier fluid, but in absence of the carrier fluid, or possibly in the presence of the silica beads, iron particles have bound to each other and the beads. The contact marks are clearly visible in the residue of the mixture and suggests that the fluid collects at these points. We believe the contact points are easier visualized because as the fluid evaporated the tension with the surface of the silica spheres collected small particles and left them behind. We also see that the surface of the spheres themselves are coated, which suggests that the contact points where the last

places to dry out. In both the ferrofluid and glycerol we see equivalent powers playing out, suggesting this is a fluid characteristic and that the size of the solid iron particles does not impact the overall forces of the dense suspension. Upon initial examination, we thought that the particles clinging to the beads might not be just ferrofluid, but damaged silica beads from the multiple impacts over the use of the beads in the experiments. If this was true, then the glycerol studies would have had small particles floating freely in the mixture as well and more thought would have to be given to the dynamics of the system having something to do with the particle fluid mixture. More images were created to address this concern and in Figure 26 we can see beads after several uses. These beads clung to the ball after impact and where washed off in a tap water container to reset for the next impact.

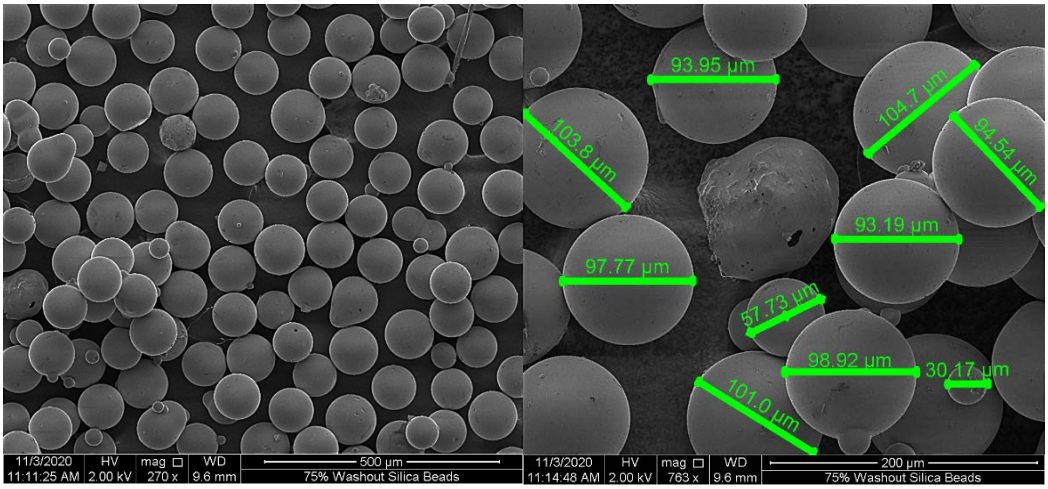

Figure 26. Used Silica Beads. Source: [19].

We see that unlike the ferrofluid mixture there is no coating observable on these particles. There are smaller beads or contaminants in the mixture, but most of the beads are within both the size specified and in spherical shape. We then compare these images to ones taken on new beads from the storage container. In Figure 27 we see that the new beads are similar in size and shape, but do have slightly less small contaminates present.

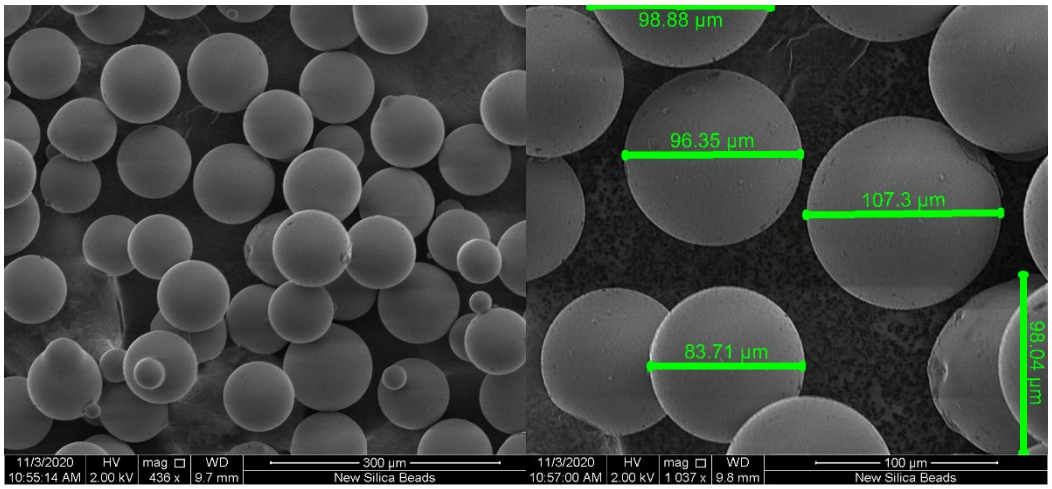

Figure 27. New Silica Beads [19].

Figures 25 through 27 suggest that our ferrofluid images are not a result of damaged beads within the fluid and the glycerol beads can be considered as a homogenous mixture of beads of a specified range in both size and shape.

Moving back to the ferrofluid mixture we then examine the size of the particles of iron with respect to the size of the beads. Again, we want to address that the ferrofluid is representative of a viscous fluid and not a particle fluid mixture. In Figure 28 we can see that at the highest image resolution available, individual groups of particles of ferrofluid are only just visible.

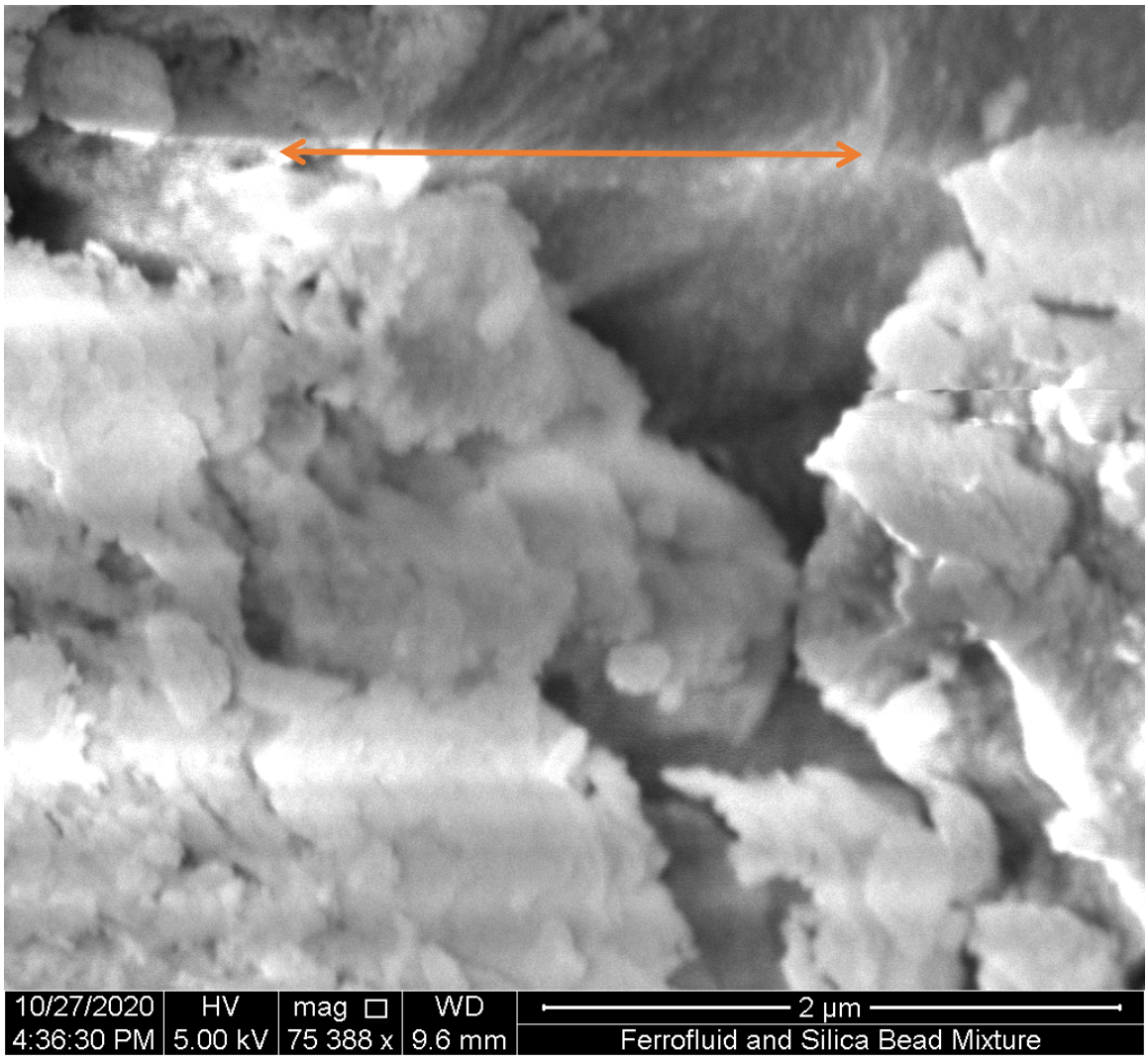

The double sided arrow represents 2,000 nanometers or 180 ferrofluid particles

Figure 28. Dry Ferrofluid Agglomeration. Source: [19].

We can see from Figure 28 that the ferrofluid particles size when compared to that of the previous images is small enough that when suspended, we believe, has no significant impact on the dynamics of the system, beyond the obvious modification of viscosity due to magnetic field. The iron particles are sufficiently small and do not interact with the relatively large glass beads. Along with the correlating data between glycerol viscosity and the range of tested ferrofluid viscosities we believe that the viscous forces are the dominant factors in this experimental design.

THIS PAGE INTENTIONALLY LEFT BLANK

V. CONCLUSION

In the work described in this thesis, we tested the feasibility of using ferrofluids in particle-fluid mixtures to create a complex fluid with macroscopic properties that could be tuned with an external magnetic field. We correlated the general behavior of particle fluid mixtures and used leading theory and experimental practice to explore the magnetoviscous effect on these systems. Calculating the expected results for rheological impact dynamics we compared both a viscous analog and ferrofluid experimental results. We explored the possibility of solid like interference from the ferrofluid mixture and addressed concerns with material limits of our experimental design.

We found that given the current prediction by Darcy-Reynolds theory and the Jerome et al. Equation [9] the values were lower than expected from [9] and even showed a trend that was opposite to the prediction: increasing viscosity leads to smaller forces in these complex fluids. To explain this counterintuitive effect, we suggest that there is a lubricating force that interferes with this model as the viscosity increases and that these lubricating values are non-trivial. We used SEM imaging on beads from different stages of the experiment and have made reasonable assumptions that the materials used performed as expected.

This discovery leads to both confirm the thesis of this paper as well as specify which applications in which these materials might be useful. If Equation (10) had held true, then by continually increasing the viscosity of a suspension the magnitude of deceleration could be altered in a way to benefit collision-based problems. However, the conclusions of this paper do suggest that tuning of this type particle-fluid mixture by use of a ferrofluid and magnetic field are possible and that there is an optimal field strength that leads to the largest forces in the material. Increasing the field strength further leads to smaller forces in the material, which could also be useful in many applications.

THIS PAGE INTENTIONALLY LEFT BLANK

LIST OF REFERENCES

[1] E. Brown, and J. Heinrich, “Shear thickening in concentrated suspensions: phenomenology, mechanisms and relations to jamming.” *Reports on Progress in Physics 77*.4 (2014): 046602.

[2] N. Causely Thesis presentation, “Impacts into saturated granular beds and dense suspensions,” Naval Postgraduate School, May 26, 2020.

[3] L. Oyarte Gálvez, S. deBeer, D. vanderMeer, and A. Pons, “Dramatic effect of fluid chemistry on cornstarch suspensions: Linking particle interactions to macroscopic rheology,” *Phys. Rev. E*, vol.95, p.030602, Mar 2017. Available: https://link.aps.org/doi/10.1103/PhysRevE.95.030602

[4] M. Wyart and M.E. Cates, “Discontinuous shear thickening without inertia in dense non-brownian suspensions,” *Phys. Rev. Lett.*, vol.112, p.098302, Mar 2014. Available: https://link.aps.org/doi/10.1103/PhysRevLett.112.098302

[5] S Odenbach, “Recent progress in magnetic fluid research.” *Journal of Physics: Condensed Matter* 16, no.32 (2004): R1135-R1150, Jul 2004. [Online]. Available: https://iopscience.iop.org/article/10.1088/0953-8984/16/32/R02/meta

[6] A. Weidner and Gräfe, Christine and von der Lühe, Moritz and Remmer, H and Clement, Joachim and Eberbeck, Dietmar and Ludwig, Frank and Müller, Robert and Schacher, F and Dutz, Silvio., “Preparation of Core-Shell Hybrid Materials by Producing a Protein Corona Around Magnetic Nanoparticles. Nanoscale research letters.” *Nanoscale Res Lett.* 2015; 10:282, Jul 2015. [Online]. Available: https://www.ncbi.nlm.nih.gov/pmc/articles/PMC4495093/

[7] M. van Hecke, “Jamming of soft particles: geometry, mechanics, scaling and isostaticity.,” *Journal of Physics.* 22(3), Jan 2010. [Online]. Available: https://doi.org/10.1088/0953-8984/22/3/033101

[8] S. R. Waitukaitis, L.K. Roth, V. Vitelli, and H.M. Jaeger, “Dynamic jamming fronts,” *EPL (Europhysics Letters)*, vol. 102, no. 4, p. 44001, May 2013. Available: https://doi.org/10.1209%2F0295-5075%2F102%2F44001

[9] J. Jerome, J. Soundar, N. Vandenberghe, and Y. Forterre, “Unifying Impacts in Granular Matter from Quicksand to Cornstarch.,” *Phys. Rev. Lett.* 117 (2016): 098003, Mar 2016. [Online]. Available: https://www.researchgate.net/publication/301855474_Unifying_Impacts_in_Granular_Matter_from_Quicksand_to_Cornstarch

[10] H. Darcy, Les fontaines publiques de Dijon ed 1856. Hachette Livre-Bnf, 2012.

[11] N. Causley, “Impact response of fluid-saturated granular beds and dense suspensions,” M.S. Thesis, Physics Department, Naval Postgraduate School, Monterey, CA, Jun 2019. Available: http://hdl.handle.net/10945/65490

[12] Ferrofluid. “Ferrofluid Product Series,” October 30, 2020 [Online]. Available: https://ferrofluid.ferrotec.com/products/

[13] R. Kaiser and R. Rosenweig, “Study of ferromagnetic liquid,” National Aeronautics and Space Administration, Washington, D.C., Aug 1969. [Online]. Available: https://www.researchgate.net/publication/24301343_Study_of_ferromagnetic_liquid

[14] R. Patel, R.V. Upadhyay, and R.V. Mehta. “Viscosity measurements of a ferrofluid: comparison with various hydrodynamic equations.” *Journal of Colloid and Interface Science* 263, no.2 (2003): 661 - 664, Jul 2003. [Online]. Available: https://doi.org/10.1016/S0021-9797(03)00325-4

[15] MO-SCI Corporation, Data sheet - GL0191 Form A1000-840 Rev 1. Available: https://mo-sci.com/wp-content/uploads/product-docs/glass-microspheres/GL0191-Data-Sheet.pdf

[16] J. Segur and H. Oberstar, “Viscosity of Glycerol and Its Aqueous Solutions,” The Miner Laboratories, Chicago 6, Ill., Sep 195. [Online]. Available: https://pubs.acs.org/doi/10.1021/ie50501a040

[17] Ferrotec Corporation, Safety data sheet for EFH Series Ferrofluid. [Online]. Available: https://ferrofluid.ferrotec.com/wp-content/uploads/sites/3/efhsds.pdf

[18] F. Da Cruz, F. Chevoir, D. Bonn, & P. Coussot, “Viscosity bifurcation in granular materials, foams, and emulsions” *Phys. Rev. E,* 66, 051305., Nov 2002. Available: https://journals.aps.org/pre/abstract/10.1103/PhysRevE.66.051305

[19] D. Grbovic, Associate Professor, Physics Department Naval Postgraduate School, Monterey CA, 2020

INITIAL DISTRIBUTION LIST

1. Defense Technical Information Center
   Ft. Belvoir, Virginia

2. Dudley Knox Library
   Naval Postgraduate School
   Monterey, California